

POLITECNICO DI TORINO

Automotive Engineering

Thesis of Master Science Degree

Study and analysis of a pneumatic spring for city cars



Academic tutor:
Prof. Giovanni Maizza

Candidate:
Victor Marco Pacini

December 2018

ABSTRACT

With the automotive field development, it has become increasingly relevant the inclusion of new technologies in a city car that improve driver and passengers' comfort and that help vehicle drivability. This project goal is to study and to analyse a pneumatic suspension capable of increasing user's comfort and improving vehicle handling by an active way. Thus, the aim is to develop a pneumatic spring that is able to replace a passive suspension mechanical spring. The new spring is based on already existing air springs for trucks and buses, though with a different design and respecting the city car constraints. The active configuration contains a pneumatic kit (compressor, air lines, valves, air tank) with a control unit. The adopted methodology includes a literature review of already existing models for an air spring and control valve, as well as the evaluation of the design parameters required for the air spring model. The simulations were done in MATLAB-Simulink and they verify the air spring alone, the air spring together with an air tank and the pneumatic system with a control valve for an active configuration. After analysing the results for the air spring alone and with the air tank, it is integrated to a quarter car active configuration so its availability in terms of sprung mass displacement can be discussed.

Keywords: air spring, pneumatic spring, pneumatic suspension, semi-active suspension, active suspension

LIST OF FIGURES

FIGURE 1 - QUARTER-CAR MODELS WITH A) ONE, B) TWO AND C) THREE DEGREES OF FREEDOM (GENTA & MORELLO, 2009)	3
FIGURE 2 - HYDRAULIC DAMPER A) TWIN TUBE B) MONOTUBE (GENTA & MORELLO, 2009)	4
FIGURE 3 - SEMI-ACTIVE MODEL (GENTA & MORELLO, 2009).....	5
FIGURE 4 - MR DAMPER (F1 DICTIONARY).....	6
FIGURE 5 - ACTIVE SUSPENSION MODELS A) WITHOUT B) WITH MECHANICAL SPRING (GENTA & MORELLO, 2009)	8
FIGURE 6 - BOSE SUSPENSION (BARATA, 2016).....	9
FIGURE 7 – SUSPENSION STRUT A) CONVENTIONAL PASSIVE B) TPMA (GYSEN, PAULIDES, JANSSEN, & LOMONOVA, 2010)	10
FIGURE 8 - COIL SPRING (SPEEDWAY MOTORS).....	11
FIGURE 9 - COIL SPRING DETAILS (MILLIKEN & MILLIKEN, 1995).....	11
FIGURE 10 - AIR SPRING TYPES ADAPTED FROM (DUNLOP).....	13
FIGURE 11 - AIR SUSPENSION COMPONENTS (AIR LIFT COMPANY)	14
FIGURE 12 - AIR SUSPENSION ASSEMBLY (PROCESS & PNEUMATICS)	15
FIGURE 13 - AIR LIFT STRUT CUT VIEW (M3 POST)	16
FIGURE 14 – AIRMATIC (LALLO, 2016)	16
FIGURE 15 - AIRMATIC STRUT MODULE ADAPTED FROM (W220 - AIRMATIC)	17
FIGURE 16 - MULTI-CHAMBER AIR SPRING (LALLO, 2016)	18
FIGURE 17 - CAVANAUGH MODEL (CAVANAUGH, 1961)	19
FIGURE 18 - BACHRACH MODEL (BACHRACH & RIVIN, 1983)	19
FIGURE 19 - EFFECTIVE DIAMETER (FIRESTONE)	20
FIGURE 20 - EFF AREA (CHANG & LU, 2008).....	21
FIGURE 21 - A EFF AND VOLUME VARIATION (CHANG & LU, 2008)	22
FIGURE 22 - FE AIR SPRING MODEL (LI, GUO, CHEN, WEIWANG, & CONG, 2013)	23
FIGURE 23 - STIFFNESS X DISPLACEMENT (A) BEFORE (B) AFTER MODIFICATION (LI, GUO, CHEN, WEIWANG, & CONG, 2013).....	23
FIGURE 24 - LEE MODEL (LEE, 2010)	24
FIGURE 25 - NONLINEAR MODEL BLOCK DIAGRAM ADAPTED FROM (QUAGLIA & SORLI, 2001)	27
FIGURE 26 - AIR SPRING BLOCK ADAPTED FROM (QUAGLIA & SORLI, 2001).....	28
FIGURE 27 - SPRUNG MASS MODEL ADAPTED FROM (CAVANAUGH, 1961)	32
FIGURE 28 – PNEUMATIC SYSTEM ILLUSTRATION (RICHER & HURMUZLU, 2000)	40
FIGURE 29 - VALVE DYNAMIC MODEL (RICHER & HURMUZLU, 2000)	41
FIGURE 30 - VALVE ORIFICE AND SPOOL DISPLACEMENT (RICHER & HURMUZLU, 2000)	42
FIGURE 31 - SIMULINK BLOCK DIAGRAM	46
FIGURE 32 - REFERENCE SPRING (A) VOLUME AND (B) EFFECTIVE AREA VARIATION	47
FIGURE 33 - SPRING AND AIR TANK MODEL.....	51
FIGURE 34 - AIR TANK MODEL WITH COMPRESSOR.....	52
FIGURE 35 - VALVE MODEL SIMULINK	53

FIGURE 36 - ACTIVE CONFIGURATION WITHOUT CONTROL VALVE	54
FIGURE 37 - ACTIVE CONFIGURATION WITH VALVE	54
FIGURE 38 - NONLINEAR MODEL STEP RESPONSE $[C] = m^3/(s \cdot Pa)$ (QUAGLIA & SORLI, 2001)	56
FIGURE 39 - IMPLEMENTED NONLINEAR MODEL STEP RESPONSE $[C] = m^3/(s \cdot Pa)$	57
FIGURE 40 - FREQUENCY RESPONSE - FORCE TRANSMISSIBILITY (QUAGLIA & SORLI, 2001)	58
FIGURE 41 - FREQUENCY RESPONSE – FORCE TRANSMISSIBILITY RESULTS	58
FIGURE 42 - FREQUENCY RESPONSE FOR THE REFERENCE QUARTER-CAR MODEL $[Rf] = Pa/(kg/s)$ (QUAGLIA & SORLI, 2001)	59
FIGURE 43 - FREQUENCY RESPONSE FOR THE IMPLEMENTED QUARTER-CAR MODEL $[Rf] = Pa/(kg/s)$	60
FIGURE 44 - SPRING PRESSURE X SPRING HEIGHT	62
FIGURE 45 - SPRING STIFFNESS X SPRING DISPLACEMENT	63
FIGURE 46 - SPRING FORCE X SPRING HEIGHT	64
FIGURE 47 - VOLUME VARIATION COMPARISON	65
FIGURE 48 - SPRING FORCE FOR DIFFERENT SPRING VOLUMES	65
FIGURE 49 - PRESSURE VARIATION ACCORDING TO DIFFERENT SPRING VOLUMES	66
FIGURE 50 - EFFECTIVE AREA VARIATION COMPARISON	67
FIGURE 51 - SPRING FORCE X SPRING HEIGHT FOR DIFFERENT VALUES OF EFFECTIVE AREA	67
FIGURE 52 - SPRING STIFFNESS X SPRING HEIGHT FOR A ROLLING DIAPHRAGM SPRING	68
FIGURE 53 - SPRING FORCE X SPRING HEIGHT FOR A ROLLING DIAPHRAGM SPRING	68
FIGURE 54 - HYSTERESIS EFFECT: STIFFNESS	69
FIGURE 55 - HYSTERESIS EFFECT: SPRING PRESSURE	70
FIGURE 56 - HYSTERESIS EFFECT: SPRING FORCE	70
FIGURE 57 - AIR SPRING INFLATION DELAY	71
FIGURE 58 - AIR SPRING INFLATION DELAY FOR DIFFERENT AIR TANK TYPES	72
FIGURE 59 - AIR TANK PRESSURE LOSS	73
FIGURE 60 - TANK FULFIL DELAY	74
FIGURE 61 - PROPORTIONAL VALVE WORKING PRINCIPLE	75
FIGURE 62 - ACTIVE SYSTEM STEP RESPONSE WITHOUT CONTROL VALVE	76
FIGURE 63 - ACTIVE CONFIGURATION STEP RESPONSE WITH VALVE	77
FIGURE 64 - AIR SUSPENSION STRUT	78

LIST OF SYMBOLS

M	Sprung mass
z	Displacement from static equilibrium
\dot{z}	Sprung mass relative speed
\ddot{z}	Sprung mass relative acceleration
h	Road input signal displacement
\dot{h}	Road input signal speed
c	Damping coefficient
k	Stiffness coefficient
β	Varying damping coefficient
c_s	Constant damping coefficient
F_d	Damping force
F_s	Spring force
F	Actuator force
p_1	Pressure inside the air spring
p_{atm}	Environment pressure
A_{eff}	Spring effective area
K_s	Spring stiffness
p_{10}	Initial air spring pressure
V_{10}	Initial air spring volume
V_1	Air spring volume
n	Polytropic coefficient
c_p	Specific heat at constant pressure
c_v	Specific heat at constant volume
x	Road signal input
\dot{m}_i	Mass airflow on the inlet
\dot{m}_e	Mass airflow on the outlet
\dot{m}	Mass airflow
m_{10}	Initial mass of air inside the air spring
ρ_1	Air density inside the air spring
R	Ideal gas constant
T_{10}	Initial air temperature inside the air spring
\dot{F}	Spring force variation
\dot{p}_1	Air spring pressure variation

\dot{A}_{eff}	Effective area variation
\dot{V}_1	Air spring volume variation
ρ_2	Air density inside the auxiliary reservoir
V_2	Auxiliary reservoir volume
V_{20}	Initial auxiliary reservoir volume
T_{20}	Initial air temperature inside the auxiliary reservoir
p_2	Pressure inside the auxiliary reservoir
p_{20}	Initial pressure inside the auxiliary reservoir
\dot{p}_2	Auxiliary reservoir pressure variation
p_i	Valve upstream pressure
p_o	Valve downstream pressure
T_{env}	Environment temperature
ρ_{atm}	Reference air density
β_{lam}	Pressure ratio at laminar flow
C	Sonic conductance
b	Critical pressure ratio
T_i	Inlet temperature of the valve
g	Gravitational acceleration
t	Time
v	Volume variation relative to spring displacement
α	Effective area variation relative to spring displacement
R_f	Linear resistance to the airflow
A_0	Initial air spring effective area
K_{V1}	Air spring volumetric stiffness
K_A	Area stiffness
K_{SV}	System stiffness
K_{V12}	Air spring plus reservoir volumetric stiffness
ω_S	Air spring natural frequency
ω_{SV}	Air spring plus reservoir natural frequency
C_i	Pneumatic capacity
C_i	Pneumatic capacity
h_0	Air spring initial height
s	Laplace variable
M_s	spool and coil assembly mass
x_s	spool displacement

x_{s0}	spring compression at the equilibrium position
c_s	viscous friction coefficient
F_f	Coulomb friction force
k_s	spool springs constant
F_c	force produced by the coil
A_v	valve effective area
x_e	effective displacement of the valve spool
R_h	orifice radius
p_w	half of spool width
n_h	number of active holes for an air path
C_f	discharge coefficient
P_{cr}	critical pressure ratio

SUMMARY

1	INTRODUCTION	1
2	STATE OF ART	2
2.1	INTRODUCTION.....	2
2.2	SUSPENSION CATEGORIES.....	2
2.2.1	<i>Passive Suspensions</i>	2
2.2.2	<i>Semi-Active Suspensions</i>	5
2.2.3	<i>Active Suspensions</i>	7
2.3	SUSPENSION SPRINGS.....	10
2.3.1	<i>Coil Springs</i>	10
2.3.2	<i>Air Springs</i>	11
2.4	PNEUMATIC SUSPENSIONS	13
2.4.1	<i>Air Suspension Components</i>	14
2.4.2	<i>Active Air Suspensions</i>	16
2.5	LITERATURE REVIEW	18
2.5.1	<i>Nonlinear model</i>	26
2.5.1.1	<i>Air Spring</i>	28
2.5.1.2	<i>Auxiliary Reservoir</i>	30
2.5.1.3	<i>Valve</i>	31
2.5.1.4	<i>Sprung Mass</i>	32
2.5.2	<i>Linearized model</i>	33
2.5.2.1	<i>Stiffness</i>	36
2.5.2.2	<i>Transfer Functions</i>	38
2.6	CONTROL VALVE	39
3	METHODOLOGY.....	45
3.1	MODEL IMPLEMENTATION	45
3.2	MODEL VALIDATION.....	47
3.3	DESIGN PARAMETERS	49
3.4	AIR SPRING AND AUXILIARY RESERVOIR	50
3.5	AIR TANK	50
3.6	CONTROL SYSTEM.....	52
4	RESULTS AND DISCUSSION	56
4.1	VALIDATION RESULTS	56
4.2	PRESSURE, FORCE AND STIFFNESS ANALYSIS.....	61
4.3	PARAMETERS ANALYSIS	64

4.3.1	<i>Volume</i>	65
4.3.2	<i>Effective Area</i>	66
4.3.3	<i>Rolling diaphragm spring</i>	68
4.4	HYSTERESIS.....	69
4.5	AIR TANK ANALYSIS.....	71
4.6	CONTROL STRATEGY: FIRST APPROACH.....	75
5	CONCLUSION	79
6	BIBLIOGRAPHY	81

1 Introduction

The comfort and performance of a vehicle greatly depends on its suspension and the improvement of these characteristics are the base for a lot of researches. In the case of a city car, driver and passenger comfort is crucial due to city road conditions and low speed situations that occur more frequently. Based on that, a lot of new technologies for vehicle suspensions have been developed to achieve a high comfort level under these conditions.

The first models of suspension were passive and for today needs they cannot give the required comfort level, especially for high end cars, however they are still used for low class vehicles. Due to the technology development today one can have semi-active and active models too, which improve substantially the vehicle comfort in comparison to the passive ones. Among the solutions used to build these new suspension models we have: electromechanical, pneumatic, hydraulic and electromagnetic solutions.

The focus of this report is on the pneumatic solution, that is already being used in some luxury cars and it is based on a pneumatic spring, a concept a long time adopted by trucks and buses. The objective of this work is to study and model a pneumatic suspension and to analyse, in a first approach, its availability for a small city car.

2 State of Art

2.1 Introduction

A vehicle suspension can be understood as a mechanism that connects the wheels to the body or to a frame attached to it, in a way that it allows the simultaneous contact of all the wheels with the ground (Genta & Morello, 2009). Among its tasks there are: to provide forces distribution and to absorb shocks received by the wheel from the road to reduce vehicle body vibrations. In this way, suspensions are essential to achieve appropriate comfort and handling levels and improvements have always been done to increase these levels.

Usually the vehicle suspensions are classified as passive, semi-active or active, depending on the elastic and damping systems. The main difference between them is the control characteristics of the system, where in the first case there are no stiffness or damping control and in the second and third cases it is possible to change these characteristics by controlling some other parameters (semi-active) or by using an external source to add an energy to the system (active).

For this project, it is important to know the functions and the types of the elastic and damping components of the suspension so, in this section, some suspension basic concepts will be introduced, and the spring component will be highlighted as it is the focus of this thesis.

2.2 Suspension Categories

The suspension classification that will be explored is the one based on the controllability of the system, then, in this section the concept of passive, semi-active and active suspensions will be introduced.

2.2.1 *Passive Suspensions*

The passive type is the simplest solution and usually it consists of spring and damper elements, as shown in Figure 1, and there is no control associated, so the suspension has its characteristics fixed.

The most common type of passive configuration is the hydraulic damper connected to a coil spring. Moreover, there are some passive systems which have limited adjustable spring or damper, however these characteristics do not automatically change according to the driving conditions.

As the suspension elastic and damping characteristics are fixed, the passive type is designed based on a type of environment disturbance expected to be the most encountered in real driving conditions, thus this type of suspension is only effective over a narrow range of road inputs. This issue of the passive solution characterizes it as the less efficient type, however, due to the design simplicity and consequently lower manufacturing and maintenance costs, when compared to other solutions, it is the cheapest one.

Nowadays, it is most used on low-end vehicles and there are researches to improve the behavior of spring and dampers individually, like the monotube or twin tube pressurized gas shocks, shown in Figure 2.

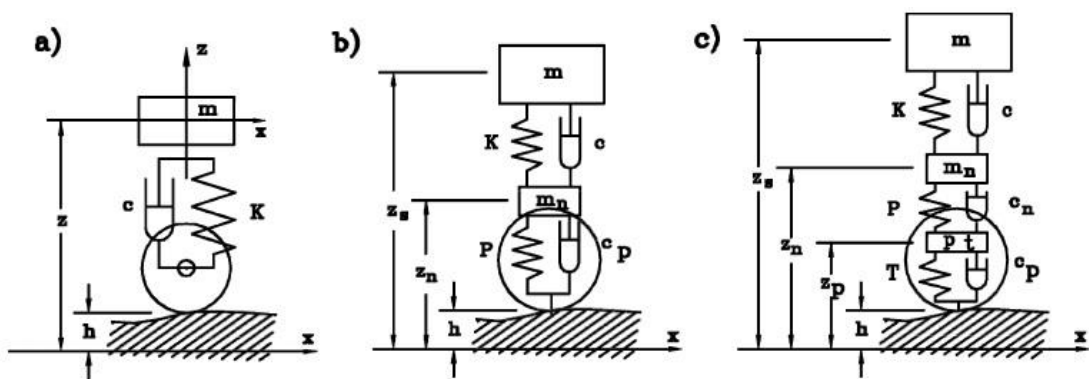


Figure 1 - Quarter-Car Models with a) one, b) two and c) three degrees of freedom (Genta & Morello, 2009)

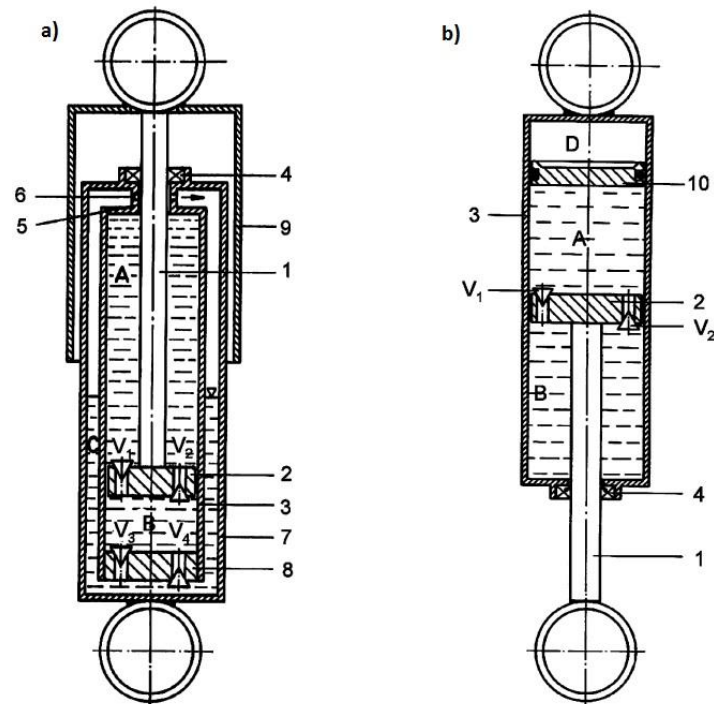


Figure 2 - Hydraulic Damper a) Twin Tube b) Monotube (Genta & Morello, 2009)

In this project the considered model will be the one degree of freedom quarter-car model, shown in Figure 1 a), in which the tire is considered as a rigid body and the only mass considered is the sprung mass. As the motions frequency range in this project is low as well as the sprung mass natural frequency (up to 3-5 Hz, range defined as ride by SAE) (Genta & Morello, 2009) this model is appropriate. The other two models are more complex, because they considerate the tire model, and they cover other frequency ranges (up to 30-50 Hz for the two degrees of freedom and up to 120-150 Hz for the three degrees of freedom), then they will not be considered in this thesis.

Then, considering the simplest case and assuming the behavior of spring and damper as linear, the equation of motion of the system can be written as:

$$M\ddot{z} + c\dot{z} + kz = c\dot{h} + kh$$

[1]

Where:

- $z(t)$ is the displacement from the static equilibrium position of the sprung mass;
- $h(t)$ is the road input;
- M is the sprung mass;
- c is the damping coefficient;
- k is the stiffness coefficient.

2.2.2 Semi-Active Suspensions

They are usually composed by a spring element and a variable damper, as shown in Figure 3. The damping coefficient can be adjustable, and it is continuously variable depending on the road conditions and being controlled by a computer algorithm. As an example, one can mention the magnetorheological damper, a type of hydraulic damper in which the viscosity of its fluid (MRF) can be changed simply by changing the magnetic field actuating on the system. Thus, by using sensors measurements, the control system can identify the road conditions and can modify the magnetic field, usually by using a electromagnetic coil, in order to obtain the best fluid viscosity for each driving situation, i.e. high viscosity (high damping) for low frequencies or low viscosity (low damping) for high frequencies.

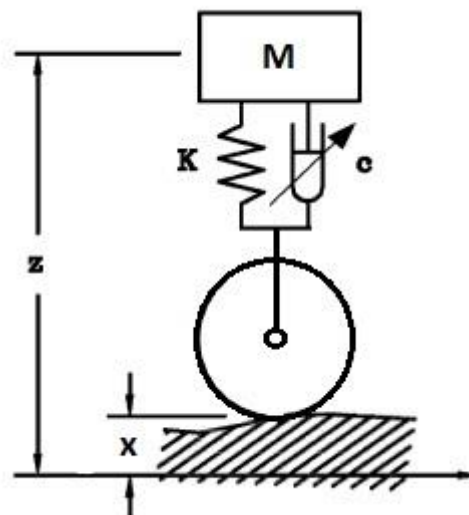


Figure 3 - Semi-Active Model (Genta & Morello, 2009)

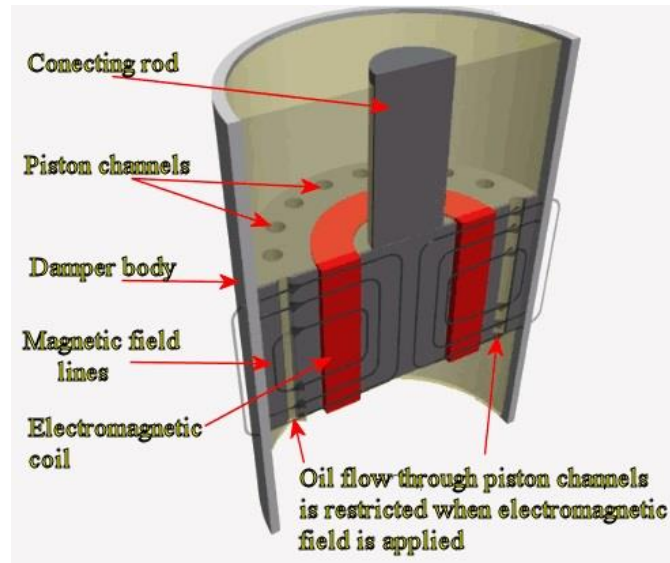


Figure 4 - MR damper (F1 Dictionary)

It is important to highlight that there is no external energy addition to the system, the controlled property is just the damping coefficient, so the semi-active type performance is limited when compared to the active type. However, this solution is cheaper and more reliable than the active one and, in terms of performance, it is more efficient than the passive one.

Considering the Figure 3 and the same assumptions of the passive linear model, the equation of motion is given by:

$$M\ddot{z} + (\beta + c_s)\dot{z} + kz = (\beta + c_s)\dot{x} + kx \quad [2]$$

Where:

- $c = (\beta + c_s)$ is the variable damping coefficient;
- β varies according to a control law;
- c_s is the constant damping coefficient;
- $x(t)$ is the road input

Rearranging the previous equation, we have:

$$M\ddot{z} + F_d + F_s = 0 \quad [3]$$

Where:

- $F_d = (\beta + c_s)(\dot{z} - \dot{x})$ is the damping force;
- $F_s = k(z - x)$ is the spring force.

So far, the assumption of linearity was accepted, i.e. the damping is only function of the velocity and the stiffness is only function of the displacement, however, it will be demonstrated later that for the air spring model, this hypothesis may be an issue.

2.2.3 Active Suspensions

It is possible to differentiate an active suspension from a semi-active one based on the control system. If it controls just the parameters of the system, for example the damping, with limited energy requirements, the system is semi-active, but if it controls the force applied by the suspension on the car body instead, usually by means of actuators which require high power consumption, the system is active (Genta & Morello, 2009).

An important parameter for active suspensions is the maximum frequency in which the system operates. If the concerned suspension working frequency is low, the system is relatively simple, however if it is high instead, it means that also the response time must be lower and the power consumption can be higher, so the system is more complex (Genta & Morello, 2009).

Usually the active suspensions are composed by a spring element and a force actuator, but theoretically, the spring and the damper could be replaced by the force actuator that would supply in this case all the force exerted between sprung and unsprung mass (Robinson, 2012) as shown in Figure 5. In active systems an algorithm is developed to control this force in real time and it is implemented in an electronic control unit that receives measurements of sensors and drives the actuator and determines the exact value of F according to a specific driving condition.

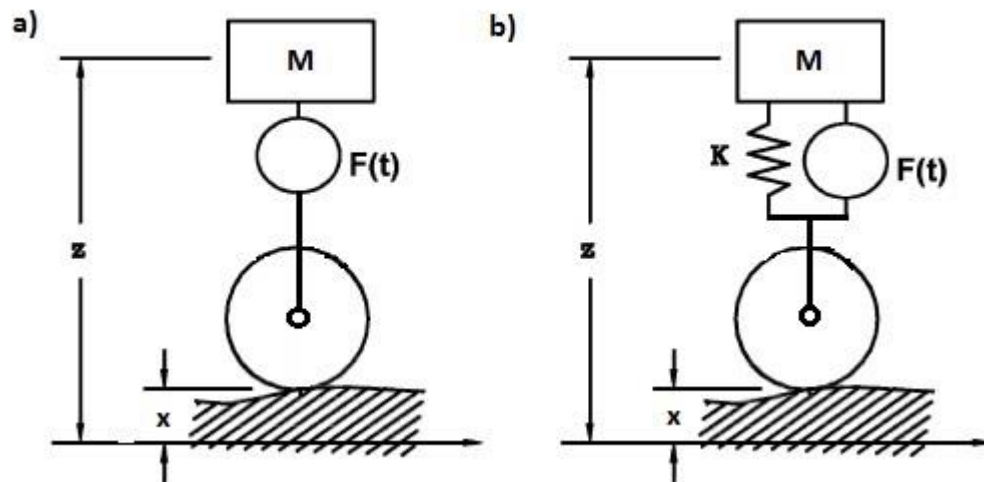


Figure 5 - Active Suspension Models a) without b) with mechanical spring (Genta & Morello, 2009)

Making the same assumption of linear model as before and considering the model of Figure 5 b), the equation of motion is given by:

$$M\ddot{z} + c_s\dot{z} + kz = c_s\dot{x} + kx + F(t) \quad [4]$$

Where:

- c_s is a damping constant that represents the inherent system damping;
- $F(t)$ is actuator force.

The active suspensions can be classified as “fully active suspension” or “high frequency active suspension” and as “slow active suspension” or “low frequency (bandlimited) active suspension”. The former classification is used to identify systems whose actuator bandwidth is less than 8 Hz and the latter is used for actuator bandwidth greater than 8 Hz (Elbeheiry, Karnopp, Elaraby, & Abdelraaouf, 1995). In this thesis the term “active suspension” includes both designations.

As examples of active suspensions applications, one can mention the hydraulic actuators (used on Active Roll Control systems) or the recent researches about electromagnetic actuators whose great representants are the innovation cases of Bose Corporation automotive suspension (Barata, 2016), shown in Figure 6, and the tubular

permanent-magnet actuator (TPMA) developed by the Eindhoven University of Technology (Gysen, Paulides, Janssen, & Lomonova, 2010), shown in Figure 7. In both cases, basically each suspension strut or also called “module” is composed by a coil spring and a linear electromagnetic motor powered by amplifiers (Ebrahimi, 2009). The system responds quickly enough to counter high frequency vibrations and can be used to control roll and pitch motions during aggressive maneuvers. Another feature of these solutions is the regenerative characteristic, when the motors act as generators and return power back through the amplifiers (Gysen, Paulides, Janssen, & Lomonova, 2010).

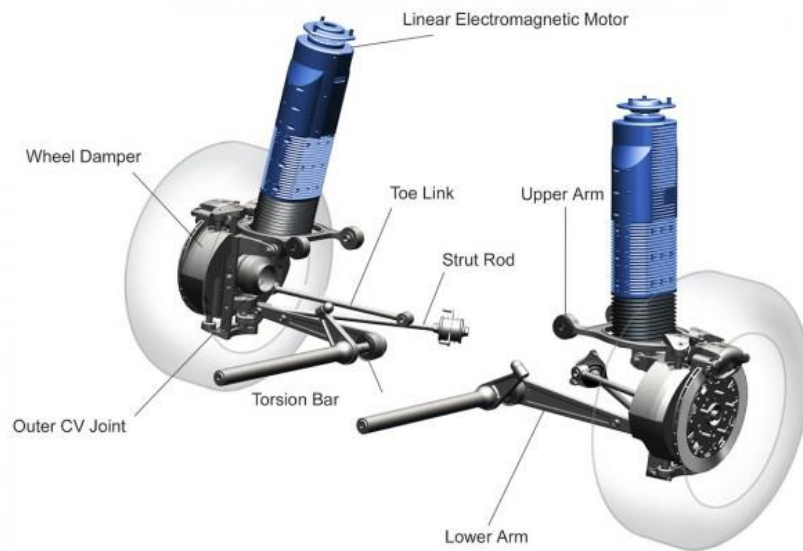


Figure 6 - Bose Suspension (Barata, 2016)

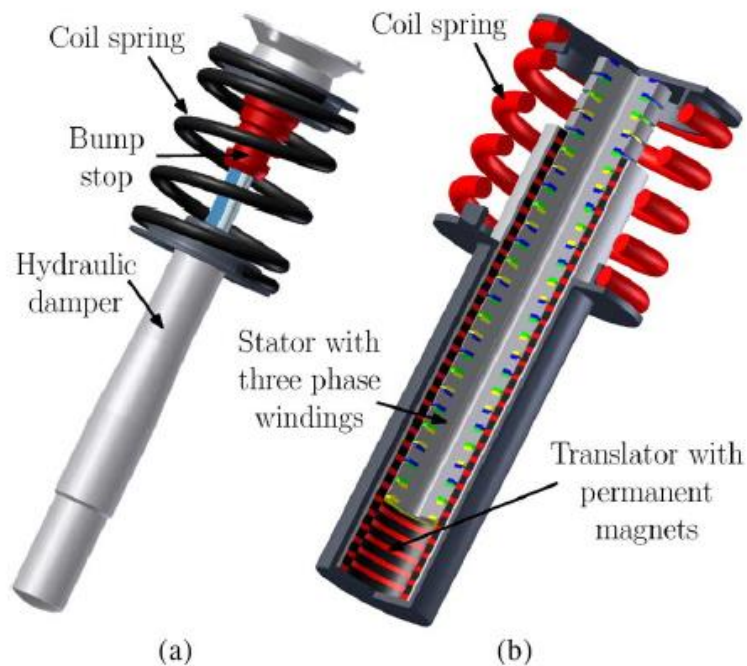


Figure 7 – Suspension Strut a) conventional passive b) TPMA (Gysen, Paulides, Janssen, & Lomonova, 2010)

2.3 Suspension Springs

The primary elastic members of the suspension are composed by springs, anti-roll bars and stop springs. In this section, the first will be discussed and some examples will be presented because is in this component that this thesis will be focused.

In (Genta & Morello, 2009) it is said that these members connect the wheel to the sprung mass elastically, store energy produced by the road profile and, moreover, they determine the body position.

In the following items some examples of springs will be shown.

2.3.1 *Coil Springs*

In (Milliken & Milliken, 1995) it is said that coil springs are the most common type of mechanical spring. They are made by a wire in torsion and its elastic properties are used to produce a linear spring rate (relationship between load and displacement, i.e. how much load is needed to obtain a certain deflection of the spring). The most common shape is the helix, as shown in Figure 8 and Figure 9, in which the main

diameter of the coil is constant, but there are also other shapes like the tapered coil (in which the main diameter varies) or coils whose wire diameter is not constant.



Figure 8 - Coil Spring (SpeedWay Motors)

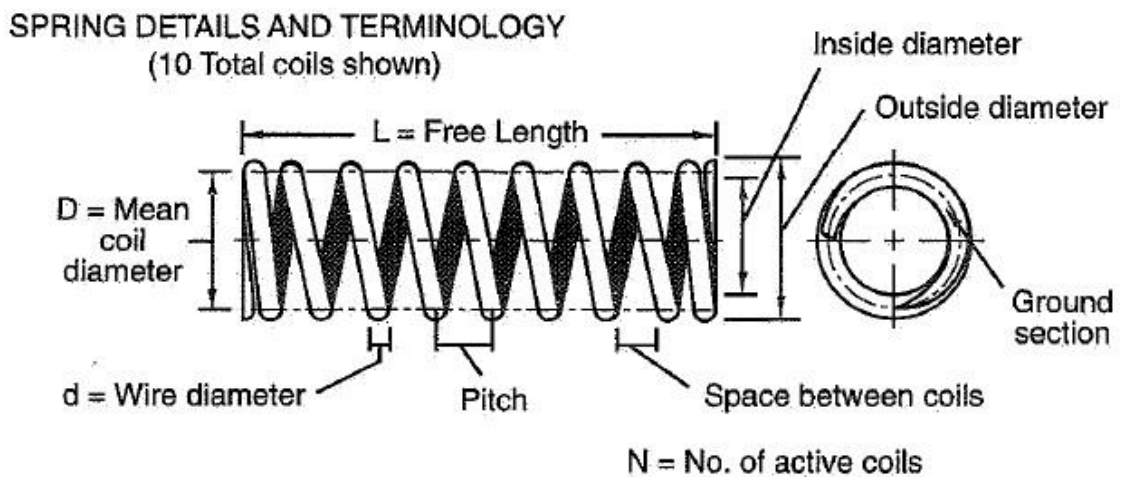


Figure 9 - Coil Spring Details (Milliken & Milliken, 1995)

2.3.2 Air Springs

According to (Genta & Morello, 2009), the air spring is similar to a tire, in which there is a rubber bellow reinforced with textile fibers containing pressurized air. It allows the vehicle trim control just by changing the inflation pressure and it improves comfort since it reduces the load excursion effect on suspension geometry. The elastic characteristic of this type of spring is provided by the air that changes its volume according to the bag pressure. Besides the elastic behavior, the air bag has a low but natural damping effect provided by the air and the rubber (Robinson, 2012).

In (Quaglia & Sorli, 2001) some advantages of air springs over mechanical springs are listed and they include:

- Adjustable load-carrying capability: if a higher load needs to be supported, the air spring pressure is increased, by adding air to the spring by means of a compressor, without changing the body height;
- Reduced weight (just considering the spring);
- Variable spring rate with constant 'tuned' frequency: when the pressure is increased due to an increasing of the supported load without significant a shift of the suspension natural frequency;
- Reduced structurally transmitted noise: due to the rubber links between the attachment points;
- Ride height variations: by inflating or deflating the air bags.

Air springs were first designed to heavy-duty vehicles (trucks, buses and trains) applications, in which they can be used on truck cabs, seat suspensions and trailer chassis suspension. However recently they are being used also for light-duty vehicles (high-end and sport cars, and mini-vans) due to the comfort and handling improvement. In this last case, the design includes an assembly between the air spring in parallel with a shock absorber, that will be later discussed in the pneumatic suspension section.

An important characteristic of the air spring is its shape, because it affects the spring rate and it is connected to load capacity, stroke length, and spring area and volume variations. Figure 10 shows some examples of air spring shapes.



Figure 10 - Air Spring Types adapted from (Dunlop)

The bags come in three main basic shapes:

- a. Convoluted bellow: This air bag normally has a larger diameter than the other types and it is used in cases of short strokes and high loads. Due to a high spring rate characteristic, this bag can provide high forces with lower pressures when compared to the other types of bags.
- b. Rolling lobe (or reversed sleeve): In comparison with the previous type, this bag has a smaller diameter and it is used for lighter loads with longer strokes. So, to provide the same force of a convoluted bellow bag, it would need a higher working pressure.
- c. Tapered sleeve: This air bag has almost the same behavior of the rolling sleeve, it has a conical shape because it is designed to fit small rooms.

Hence, choosing the bag shape for an air suspension project will depend basically on the required stroke length, the load to be supported and the available room for the spring.

2.4 Pneumatic suspensions

Pneumatic suspensions are systems in which air springs are the main elastic element and they may act as passive, semi-active or active suspensions. The advantages of using an air suspension are those from the air springs, where the levels of comfort, handling and ride height are controllable.

2.4.1 Air Suspension Components

For this type of suspension, besides the air springs, we must also consider all the components included in the system, as shown in Figure 11, because they will impact on the sprung mass, the available room, and the final price of the vehicle. The assembly is shown by Figure 12 and the list of the main components is:

- air tank;
- air compressor;
- airlines;
- electrical harshness;
- sensors and valves;
- Electronic Control Unit (ECU).



Figure 11 - Air Suspension Components (Air Lift Company)

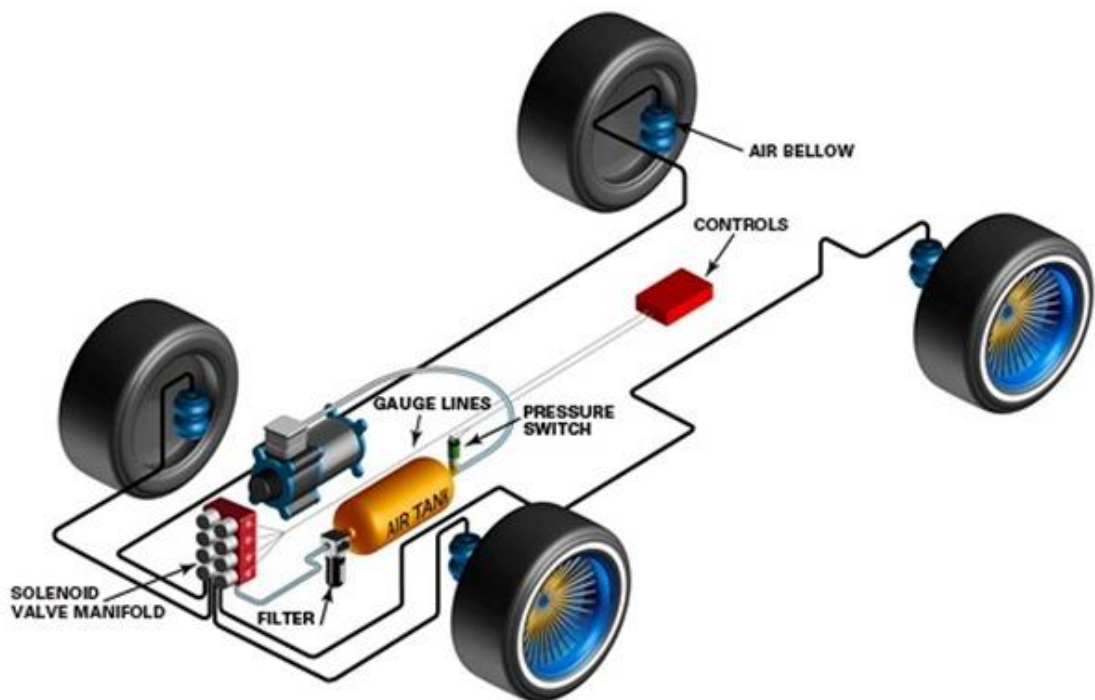


Figure 12 - Air Suspension Assembly (Process & Pneumatics)

In the case of a passive suspension, the working principle is the following: the air compressor works to maintain a specified pressure level in the tank, which is connected to the air springs by the airlines and valves. When the driver wants to change the ride height or the suspension stiffness he manually commands the ECU that send a sign to the valves, by means of the electrical harshness, and so they can be closed or opened according to the driver setup. By doing so, the valves that connect the air tank to the air springs control the inflation or deflation of the bags, and so the ride height or the spring stiffness can be changed.

Air suspensions are very common used on heavy-duty vehicles, but recently they are being used also in high-end cars and sport cars and, in this case, it is common to find the air springs assembled in parallel with a damping device (usually a hydraulic damper) in the same strut, as shown in Figure 13.



Figure 13 - Air Lift Strut Cut View (M3 Post)

2.4.2 Active Air Suspensions

The idea of the active pneumatic suspensions is to use the air spring both as a spring and as an actuator (Sharp & Hassan, 1988). So, in this case the air spring is responsible for the force generation and it requires real time pressure control, as known as pneumatic vibroisolation. This methodology of vibration control is based on pressure variation inside the air spring chamber to reduce the sprung mass acceleration.

Among the available active air suspensions on the market we can mention the AIRMATIC solution made by Mercedes-Benz, shown in Figure 14.



Figure 14 – AIRMATIC (Lallo, 2016)

This solution combines a pneumatic suspension with an Adaptive Damping Control (ADS). The former controls the vehicle ride height and suspension stiffness, and its air springs can work as actuators together with the previous mentioned air suspension components, and the latter is responsible for the variable damping provided by a hydraulic damper (Lallo, 2016). Figure 15 shows an AIRMATIC front suspension module.

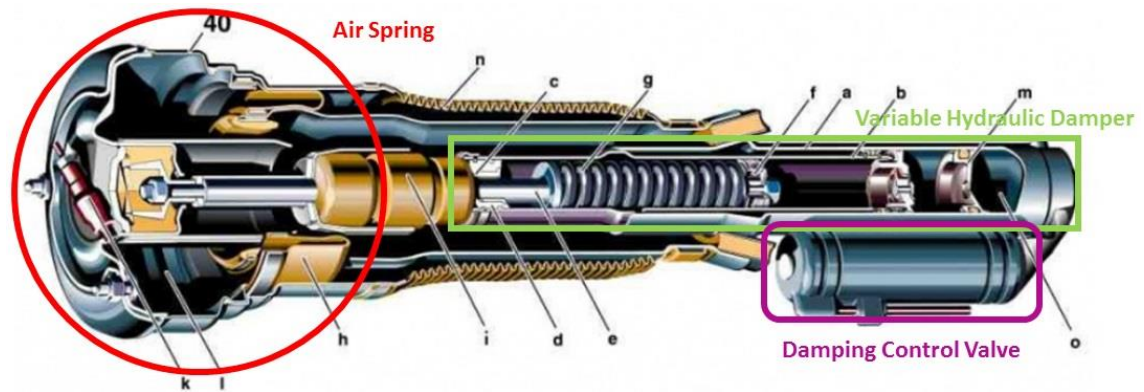


Figure 15 - AIRMATIC strut module adapted from (W220 - Airmatic)

In (W220 - Airmatic), the AIRMATIC solution is explained. As an active system, besides the suspension components are the same from the passive one, the working principle is different, in this case the sensors make real time measurements and send the information to the ECU that can control the valves to control the stiffness of the springs as well as the damping properties of the hydraulic damper. Then, except for a setup defined by the driver, the suspension control can be done depending on the road conditions, i.e. for rough roads a configuration with soft springs can be chosen by deflating the springs to turn them softer and by controlling the Damping Control Valve, improving comfort, instead for highways it is possible to adopt a configuration with stiffer springs and higher damping to improve the handling.

For the rear suspension, Mercedes developed a multi-chamber air spring, as shown in Figure 16. In this assembly the air spring and the damper are separated, and the bag has three chambers that can be opened or closed according to driving conditions or predefined chosen setups. The idea relies on the fact that by opening or closing the valves that connect the auxiliary chambers to the main chamber it is

possible to change the spring stiffness and to provide some damping, as will be demonstrated later in this thesis.

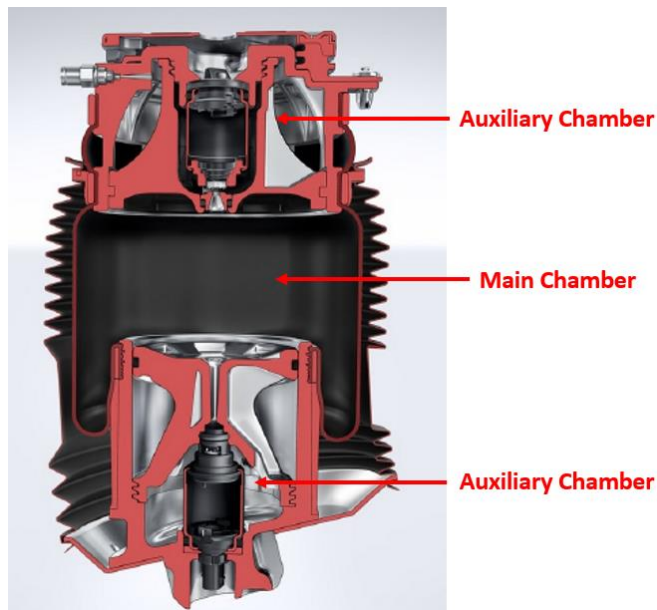


Figure 16 - Multi-Chamber Air Spring (Lallo, 2016)

2.5 Literature Review

This project is focused in the concept of multi-chamber spring, so it will be presented a study of a spring connected to an auxiliary reservoir, that provides adaptive stiffness, by means of an orifice valve that provides fluidic resistance, i.e. damping, for vibration control. Considering this concept of air suspension as a pneumatic vibration isolator, the model that will be utilized in this thesis is the one presented by (Cavanaugh, 1961), showed by Figure 17, which has been used by many other works, for example (Bachrach & Rivin, 1983), (Quaglia & Sorli, Air Suspension Dimensionless Analysis and Design Procedure, 2001), (Esmailzadeh, 1978) and (Toyofuku, Yamada, Kagawa, & Fujita, 1999). In this section some interesting works about air springs will be quickly presented because this thesis is based on some hypothesis or ideas from these authors. Moreover, sometimes the term “spring” will be used for matter of simplicity and it makes reference to the air spring, if the mentioned spring would be a coil spring, the term “mechanical spring” will be used instead.

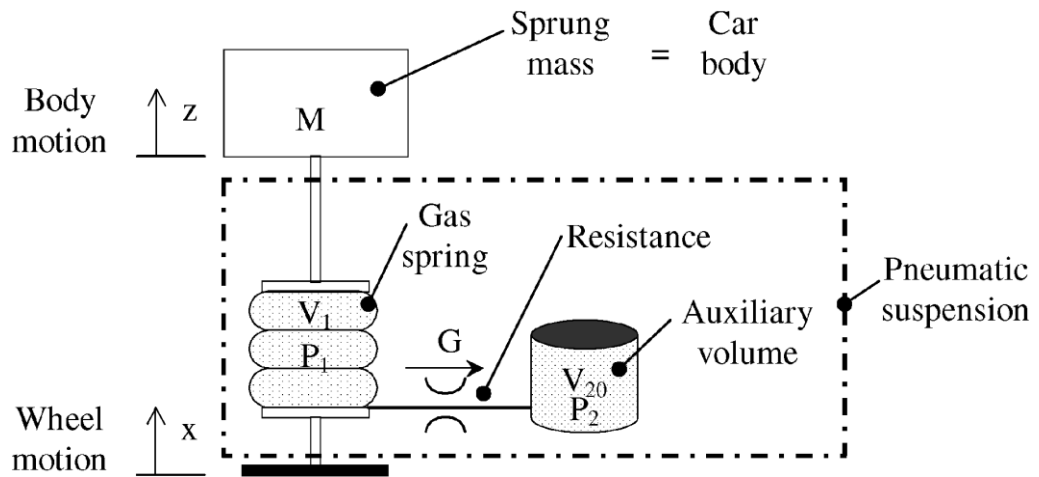


Figure 17 - Cavanaugh Model (Cavanaugh, 1961)

In 1983 (Bachrach & Rivin, 1983) showed a model with this configuration, as shown in Figure 18, in which the resistance was capillary and presented the behavior of a damped air spring as well as the loss factor that depends only on the relation between the reservoir and spring volumes. He also demonstrated that by changing the values of the flow resistance the frequency in which the maximum damping occurs also changes. With a similar model, (Toyofuku, Yamada, Kagawa, & Fujita, 1999) studied the effects of the length of the pipe between the reservoir and the spring.

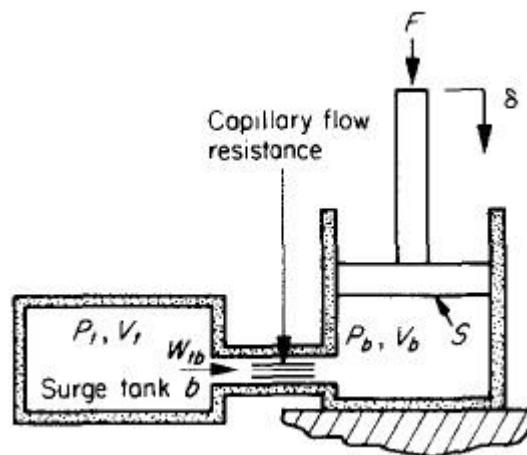


Figure 18 - Bachrach Model (Bachrach & Rivin, 1983)

(Chang & Lu, 2008) presented in 2008 a study in which a new air spring model was tested in comparison to a traditional one, without an auxiliary reservoir in this case. Moreover, he did experimental tests with two air springs (one from a SUV and another from a truck) to compare with simulation results to validate his model. After that he

integrated the model into a full-vehicle multi-body dynamic model and did some simulations in ADAMS and MATLAB/Simulink in order to investigate the full-vehicle characteristics with air spring suspensions. In (Chang & Lu, 2008) work, it was presented also the importance of the geometric parameters of the air spring so, at this point, the concepts of the air spring effective area (A_{eff}) and volume will be presented.

According to (Firestone), the effective area is the air spring area which carries the load and its diameter is determined by the distance between the centres of the radius of curvature of the air spring loop that can be approximated by a circle. Figure 19 shows the effective diameter for different shapes of air spring.

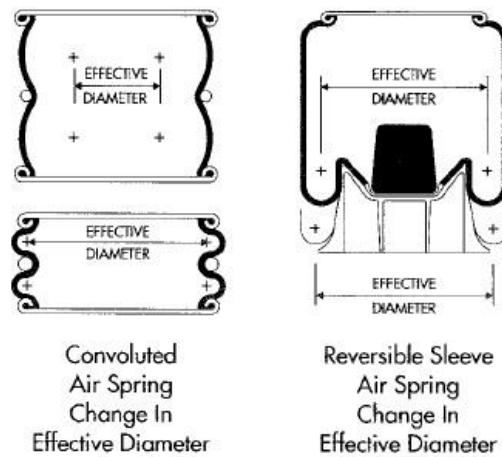


Figure 19 - Effective Diameter (Firestone)

The effective area can be calculated by using the effective diameter, as demonstrated in the next equation:

$$A_{eff} = \pi \frac{d^2}{4} \quad [5]$$

It was demonstrated in the literature (Quaglia & Sorli, Experimental And Theoretical Analysis Of An Air Spring With Auxiliary Reservoir, 2000) that the effective area depends on the spring deflection and on the bag pressure, however the latter contribution could be considered negligible. Thus, when the spring is compressed or extended, independently on the pressure, the effective diameter changes, and so does the effective area. (Chang & Lu, 2008) presents some experimental tests with some

different spring shapes and how the effective area can vary according to a deflection of the spring, as shown in Figure 20.

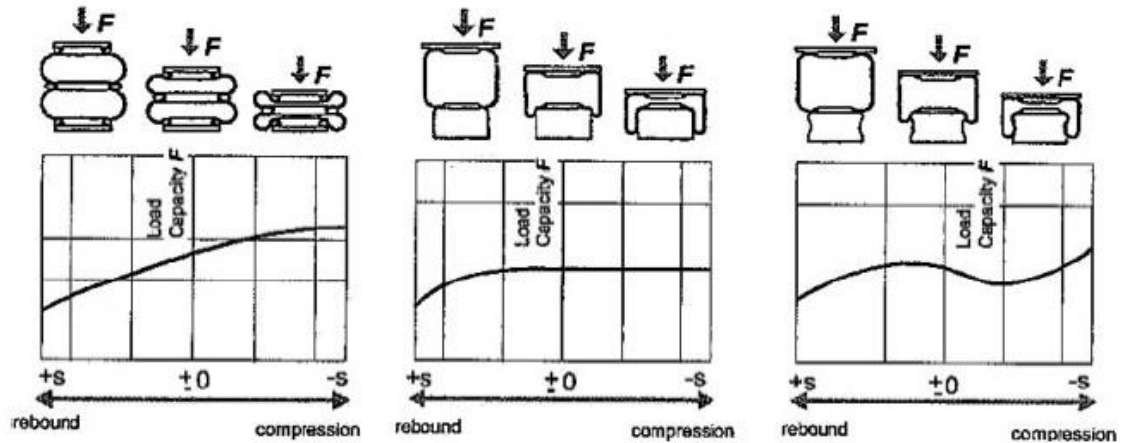


Figure 20 - Eff Area (Chang & Lu, 2008)

The force applied by the air spring is calculated by the following equation:

$$F = (p_1 - p_{atm})A_{eff} \quad [6]$$

Where:

- p_1 is the pressure inside the air spring;
- p_{atm} is the environment pressure;
- A_{eff} is the effective area.

From the previous equation and by analyzing Figure 20 it is possible to notice that the choose of the air spring shape is crucial to determine the spring force behavior.

Another important geometric parameter is the air spring volume that also does not depends on the bag pressure, just the spring length. Usually the volume and the effective area characteristics over spring deflection, showed by Figure 21, are experimentally determined (the data is given by the manufacturers) or it can be calculated by the geometric shape of the spring and piston (Winnen, 2005).

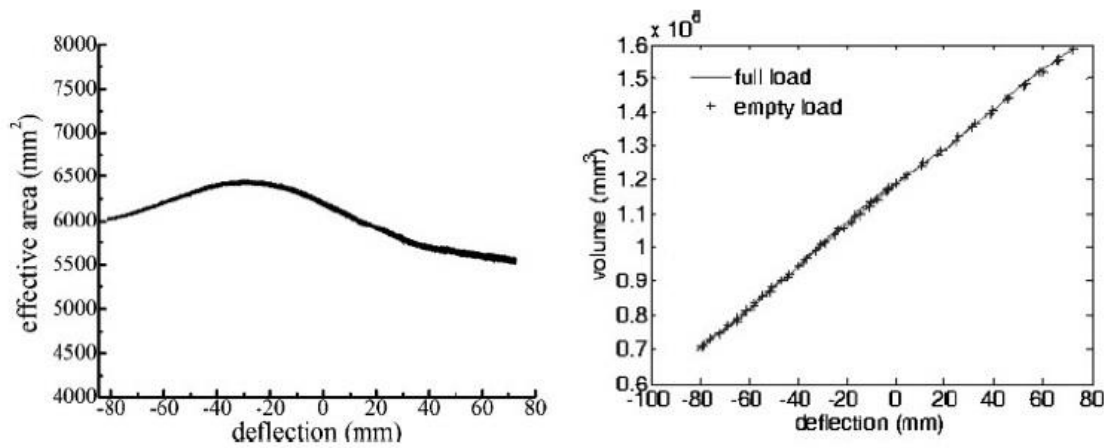


Figure 21 - A_{eff} and Volume variation (Chang & Lu, 2008)

The effective area and volume variation are related to the spring shape, then to change these parameters one must change the geometry of the spring. This is not an easy task since the spring shape is a complex issue to deal due to the rubber component presence and sometimes the shape variation can be different from the ones shown in Figure 21. To demonstrate the influence of the spring geometry, (Li, Guo, Chen, WeiWang, & Cong, 2013) did a Finite Element (FE) analysis to determine the effective area in which he changed the geometry of his spring model to achieve his project required stiffness. The model of the spring is shown by Figure 22 and the stiffness simulation results are shown by Figure 23.

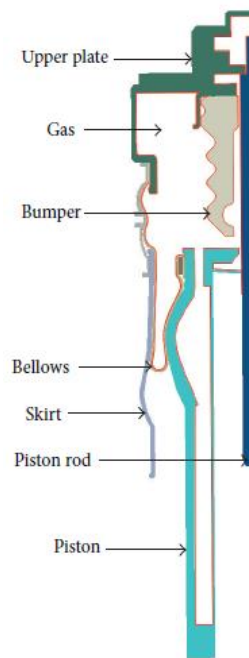


Figure 22 - FE air spring model (Li, Guo, Chen, WeiWang, & Cong, 2013)

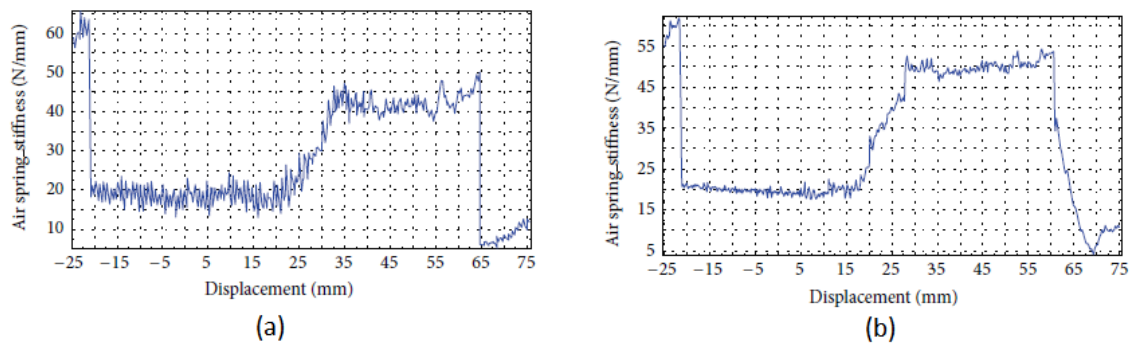


Figure 23 - Stiffness \times Displacement (a) before (b) after modification (Li, Guo, Chen, WeiWang, & Cong, 2013)

The experimental tests were done in a static stiffness machine and the geometry modifications were done aiming to reach the required stiffness: 20 N/mm in low stiffness area and 50 N/mm in high stiffness area. Figure 22 shows the design of this air spring that is involved in a shell that models the spring shape during compression, so it is possible to define the spring deformation and so, the required effective area.

Most of the studies about the dynamic behavior of an air spring includes the effective area and volume variations experimental tests for the spring force calculation. After doing these tests and by adopting a thermodynamic model, (Lee, 2010) modelled an air spring without external reservoir and flow resistance taking into account the heat

exchange between the bag and the environment, as shown in Figure 24. Other works present the influence of the heat exchange, but for gas springs, for example in (Kornhauser & Smith, 1993). Also, in (Lee, 2010) model, he considers that the mass inside the spring changes, so he studies the effects of the hysteresis in the air spring. He concludes that, from his model, the hysteresis occurs mainly by the heat exchange, however, we will see that, in the model that includes air spring plus orifice valve and reservoir, there is also the hysteresis effect even considering no heat exchange hypothesis.

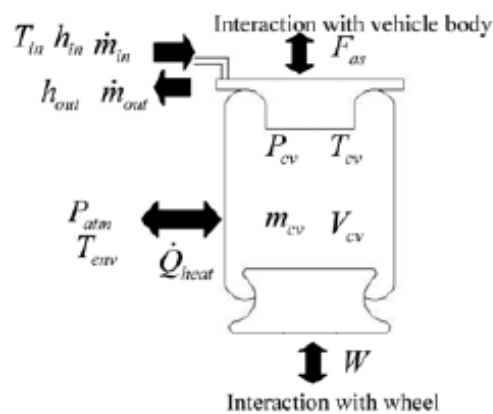


Figure 24 - Lee Model (Lee, 2010)

In 2000 (Quaglia & Sorli, Experimental And Theoretical Analysis Of An Air Spring With Auxiliary Reservoir, 2000) studied the air spring design parameters and its geometry and how they affect static and dynamic performance. In this work he presents the effective area and volume variations as function of spring deflection and how they affect the stiffness. So, the following equations are presented by (Quaglia & Sorli, Experimental And Theoretical Analysis Of An Air Spring With Auxiliary Reservoir, 2000) to calculate the spring stiffness.

The spring stiffness is given by:

$$K_s = -\frac{F}{h} \quad [7]$$

Where:

- F is the spring force;
- h is the spring deflection.

Deriving this expression, we have:

$$K_s = -\frac{dF}{dh} \quad [8]$$

So, from equation [6] and [8] it is possible to write:

$$K_s = -\left(\frac{dp_1}{dh} A_{eff} + (p_1 - p_{atm}) \frac{dA_{eff}}{dh}\right) \quad [9]$$

Air is considered an ideal gas and when the air spring compresses or extends the air is submitted to a polytropic transformation then, according to (Moran & Shapiro, 2006), we have:

$$p_{10} V_{10}^n = p_1 V_1^n \quad [10]$$

Where:

- p_{10} is the initial pressure of the air spring;
- V_{10} is the initial volume of the air spring;
- p_1 is the air spring pressure at the instant $t > 0$;
- V_1 is the air spring volume at the instant $t > 0$;
- n is the polytropic coefficient (for an ideal gas it is defined as $n = \frac{c_p}{c_v}$);
- c_p is the specific heat at constant pressure;
- c_v is the specific heat at constant volume.

So, if we derive the previous equation we can obtain the pressure variation in function of spring height variation:

$$\frac{dp_1}{dh} = \frac{np_{10}V_{10}^n}{V_1^{n+1}} \cdot \frac{dV_1}{dh} \quad [11]$$

Hence, substituting [11] in [9] the stiffness equation is obtained:

$$K_s = -\frac{np_{10}V_{10}^n A_{eff}}{V_1^{n+1}} \cdot \frac{dV_1}{dh} - (p_1 - p_{atm}) \frac{dA_{eff}}{dh} \quad [12]$$

From the previous equation it can be noticed that the spring stiffness depends on the volume variation and the effective area variation. Also, if we increase the volume of the spring, the stiffness will reduce and if we increase the pressure inside the spring, the stiffness will increase. These properties can be explored to a future control methodology in which is possible to control the suspension stiffness to adapt the vehicle to certain road conditions to improve comfort or handling.

In 2001 (Quaglia & Sorli, 2001) continued the previous study and, based on the model proposed by (Cavanaugh, 1961), he analyses the self-damping behavior of the system as well as he proposes a dimensionless model for air spring design. The analytical analysis presented in this thesis is based on that already proposed by (Cavanaugh, 1961) and adapted by (Quaglia & Sorli, 2001), and in the next lines the developed mathematical model will be shown.

2.5.1 Nonlinear model

It starts with a nonlinear model in which a quarter car model is used with basically two main systems: the sprung mass (i.e. the vehicle body) and the suspension (composed by the air spring, the fluid resistance, and the auxiliary reservoir). Figure 25 shows the MATLAB-Simulink block diagram implemented model.

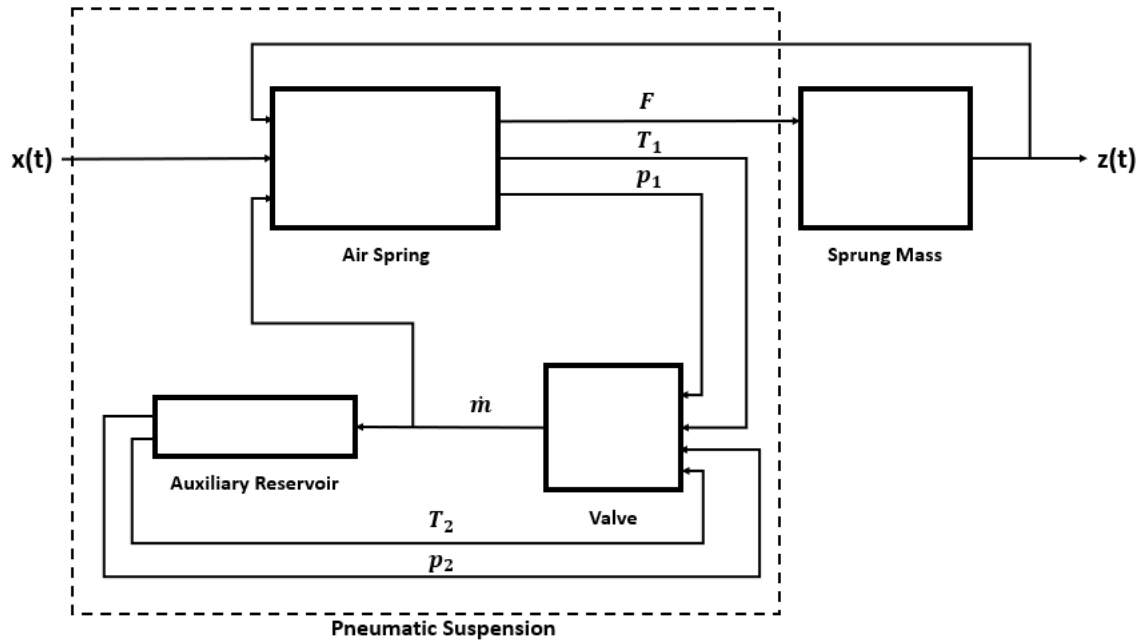


Figure 25 - Nonlinear model block diagram adapted from (Quaglia & Sorli, 2001)

In the model $z(t)$ and $x(t)$ represent the sprung mass and the wheel displacements respectively. The simulations were done by using an input $x(t)$ that simulates the road profile and the body displacement $z(t)$ was calculated by using the body equation of motion and the spring force generated $F(t)$. For the suspension system, the output $F(t)$ depends on the relative movement between the wheel and the sprung mass, i.e. the suspension deformation $z(t) - x(t)$, regardless the suspension type.

The suspension system is divided in three subsystems: the air spring, the valve and the auxiliary reservoir. In the air spring subsystem, we have the road input and spring force output. The last is calculated by using the spring deflection as already mentioned but also depends on the pressure inside the spring (p_1) as well as the air mass flow rate (\dot{m}) between the bag and the reservoir. Thus, p_1 needs to be calculated and it is used also to calculate \dot{m} , so it is used as an output of the air spring subsystem and as an input to the valve one. In the last the air flow rate is given by the pressure difference between the bag and the reservoir, so it receives as input the pressures p_1 and p_2 and gives \dot{m} , which will act as an input to the bag and the reservoir, so the air mass inside the spring and the reservoir can be calculated to close the loop for the pressures calculation as it will be demonstrated.

2.5.1.1 Air Spring

The air spring block diagram is given by the Figure 26:

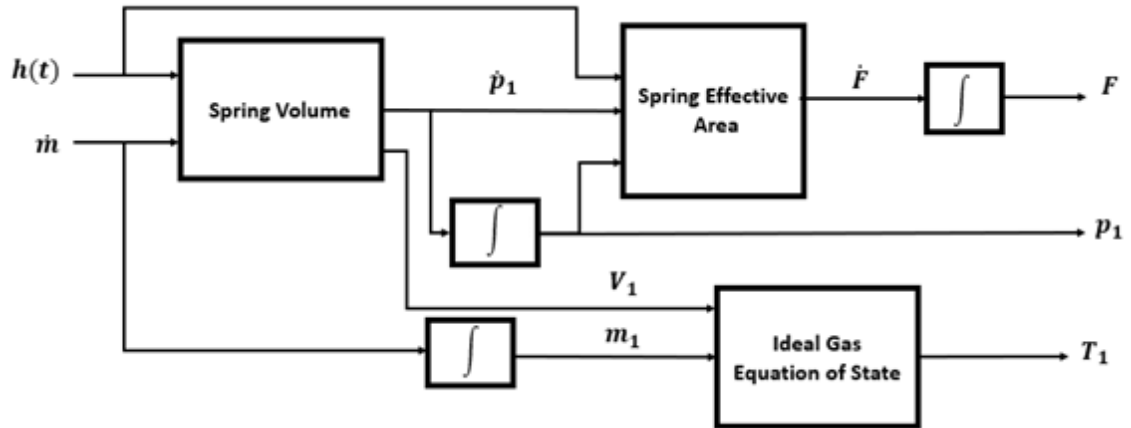


Figure 26 - Air Spring block adapted from (Quaglia & Sorli, 2001)

For this model the hypothesis of no heat exchange between the air spring and the environment was adopted. Analyzing the air spring control volume and applying the continuity equation we have:

$$\frac{dm_{cv}}{dt} = \sum \dot{m}_i - \sum \dot{m}_e = -\dot{m} \quad [13]$$

Where:

- \dot{m}_i is the airflow on the inlet;
- \dot{m}_e is the airflow on the outlet.

As the model considers just a single connection between the air spring and the reservoir the following assumption is made:

- $\dot{m} > 0$ air is entering the spring;
- $\dot{m} < 0$ air is leaving the spring

Hence, one can write the airflow equation as:

$$\dot{m} = -\frac{d(\rho_1 V_1)}{dt} = -V_1 \frac{d\rho_1}{dt} - \rho_1 \frac{dV_1}{dt} \quad [14]$$

The air density is defined by:

$$\rho_1 = \frac{m_{10}}{V_1} \quad [15]$$

In which m_{10} is the initial air mass inside the spring.

From the ideal gas equation of state, we have:

$$pV = mRT \quad [16]$$

By substituting the equations [16] and [10] in [15] we have:

$$\rho_1 = \frac{p_{10}}{RT_{10}} \cdot \left(\frac{p_1}{p_{10}}\right)^{\frac{1}{n}} \quad [17]$$

Deriving the previous equation and substituting it in equation [14] we can write the pressure gradient equation as:

$$\dot{p}_1 = -\frac{nRT_{10}}{V_1} \left(\frac{p_1}{p_{10}}\right)^{\frac{n-1}{n}} \dot{m} - \frac{np_1}{V_1} \dot{V}_1 \quad [18]$$

As explained before, the variation of the spring volume and the spring area are just function of the spring height which varies in time, so one can write:

$$V_1 = V_1(h(t)) \quad [19]$$

$$A_{eff} = A_{eff}(h(t)) \quad [20]$$

Still in the spring block, besides the temperature T_1 being given by equation [16] there is also the calculation of the derivative of the spring force by using the equation [6]:

$$\dot{F} = \dot{p}_1 A_{eff}(h(t)) + (p_1 - p_{atm}) \dot{A}_{eff}(h(t)) \quad [21]$$

By integrating the previous expression is possible to calculate the spring force F .

2.5.1.2 Auxiliary Reservoir

The reservoir model follows the same methodology as the air spring, however the volume V_{20} in this case is constant and so the equation of the pressure gradient \dot{p}_2 is simpler as it will be demonstrated.

Using the continuity equation, we can write the airflow expression as:

$$\dot{m} = \frac{d(\rho_2 V_2)}{dt} = \frac{d\rho_2}{dt} V_2 \quad [22]$$

One can notice that in this case the airflow is positive and means that the air is entering the auxiliary reservoir.

From the air density equation and its derivative, the pressure gradient is given by:

$$\dot{p}_2 = \frac{nRT_{20}}{V_2} \left(\frac{p_2}{p_{20}} \right)^{\frac{n-1}{n}} \dot{m} \quad [23]$$

2.5.1.3 Valve

The connection between the spring and the auxiliary reservoir is modelled as a Constant Area Pneumatic Orifice according to ISO 6358, that considers a flow rate of an ideal gas through a fixed-area sharp-edged orifice. It is based on (Sanville, 1971) equations and is used by (Quaglia & Sorli, 2001).

The standard considers the laminar, subsonic and choked flow, and its equations are:

$$\dot{m} = \begin{cases} k_1 p_i \left(1 - \frac{p_o}{p_i}\right) \sqrt{\frac{T_{env}}{T_i}} \text{sign}(p_i - p_o) & \text{if } \frac{p_o}{p_i} > \beta_{lam} \text{ (laminar)} \\ p_i C \rho_{atm} \sqrt{\frac{T_{env}}{T_i}} \sqrt{1 - \left(\frac{p_o - b}{1 - b}\right)^2} & \text{if } \beta_{lam} > \frac{p_o}{p_i} > b \text{ (subsonic)} \\ p_i C \rho_{atm} \sqrt{\frac{T_{env}}{T_i}} & \text{if } \frac{p_o}{p_i} \leq b \text{ (choked)} \end{cases} \quad [24]$$

$$k_1 = \frac{1}{1 - \beta_{lam}} C \rho_{atm} \sqrt{1 - \left(\frac{\beta_{lam} - b}{1 - b}\right)^2} \quad [25]$$

Where:

- p_i is the inlet (upstream) pressure of the valve;
- p_o is the outlet (downstream) pressure of the valve;
- T_{env} is the reference temperature (environment temperature);
- ρ_{atm} is the reference air density (in which the sonic conductance was measured);
- β_{lam} is the pressure ratio at laminar flow;

- C is the sonic conductance and according to (Beater, 2007) it can be written as $C = 0.128 \cdot 10^{-8} \cdot d^2$ in which d is the orifice diameter given in [mm] and C is given in $m^3/(s \cdot Pa)$;
- b is the critical pressure ratio;
- T_i is the inlet temperature of the valve.

2.5.1.4 Sprung Mass

Considering the one degree of freedom quarter car model, as shown in Figure 27, the equation of motion of the sprung mass is given by:

$$M\ddot{z} + Mg - F = 0 \quad [26]$$

Where:

- \ddot{z} is the sprung mass acceleration;
- M is the sprung mass;
- g is the gravitational acceleration;
- F is the spring force.

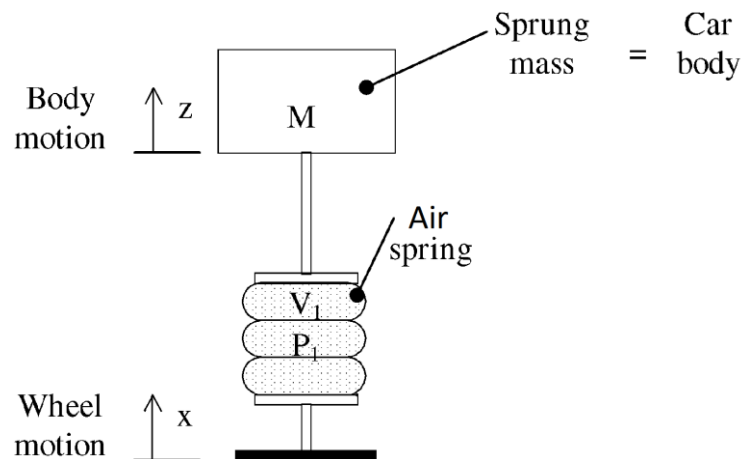


Figure 27 - Sprung Mass Model adapted from (Cavanaugh, 1961)

The equations that describe the system working are [18], [23], [21], [24] and [26].

2.5.2 Linearized model

In order to further analyze a frequency response of the system and, in a future research, to be able to implement a control system to a possible active air spring, a linearization is done. In this way, by using a Taylor Series expansion of the previous equations considering that the equilibrium point is the initial height h_0 of the spring is possible to obtain a linearized model.

At the equilibrium point the values of the variables are:

- $\dot{m}|_{h_0} = \dot{m}|_{h_0} = 0;$
- $p_1|_{h_0} = p_{10};$
- $p_2|_{h_0} = p_{20};$
- $\dot{p}_1|_{h_0} = 0;$
- $\dot{p}_2|_{h_0} = 0;$
- $V_1|_{h_0} = V_{10};$
- $V_2|_{h_0} = V_{20};$
- $\dot{V}_1|_{h_0} = 0;$
- $h|_{h_0} = h_0;$
- $\dot{h}|_{h_0} = 0;$
- $A_{eff}|_{h_0} = A_0;$
- $\left. \frac{dV}{dh} \right|_{h_0} = \nu;$
- $\left. \frac{dA_{eff}}{dh} \right|_{h_0} = \alpha.$

The linearization method basically consists in writing a nonlinear continuous function by means of a Taylor series around an operating point, as shown in (Ogata, 2002). Thus, the expansion of a function with n inputs that considers just the first order terms is given by the following equation:

$$\begin{aligned}
f(x_1, x_2, \dots, x_n) &= f(\bar{x}_1, \bar{x}_2, \dots, \bar{x}_n) + \frac{\partial f}{\partial x_1}(x_1 - \bar{x}_1) + \frac{\partial f}{\partial x_2}(x_2 - \bar{x}_2) + \dots \\
&+ \frac{\partial f}{\partial x_n}(x_n - \bar{x}_n)
\end{aligned} \tag{27}$$

Where:

- x_1, x_2, \dots, x_n are the inputs;
- $\bar{x}_1, \bar{x}_2, \dots, \bar{x}_n$ are the values of the variables at the operation point.

Therefore, by applying this methodology to the equation [18] it becomes:

$$\dot{p}_1 = -\frac{nRT_{10}}{V_{10}}\dot{m} - \frac{np_{10}}{V_{10}}\dot{V}_1 \tag{28}$$

We can write \dot{V}_1 as:

$$\dot{V}_1 = \left. \frac{dV}{dh} \right|_{h_0} \frac{dh}{dt} = v \cdot \dot{h} \tag{29}$$

Hence, the linearized spring pressure gradient is given by:

$$\dot{p}_1 = -\frac{nRT_{10}}{V_{10}}\dot{m} - \frac{np_{10}v}{V_{10}}\dot{h} \tag{30}$$

Now, applying the same to equation [21]:

$$\dot{F} = \dot{p}_1 A_0 + (p_{10} - p_{atm}) \dot{A}_{eff} \tag{31}$$

Where \dot{A}_{eff} can be written as:

$$\dot{A}_{eff} = \left. \frac{dA}{dh} \right|_{h_0} \frac{dh}{dt} = \alpha \cdot \dot{h} \quad [32]$$

So, the linearized spring force variation is given by:

$$\dot{F} = \dot{p}_1 A_0 + (p_{10} - p_{atm}) \alpha \dot{h} \quad [33]$$

Analogously to [30], the linearized expression for the reservoir pressure is given by:

$$\dot{p}_2 = \frac{nRT_{20}}{V_{20}} \dot{m} \quad [34]$$

According to (Quaglia & Sorli, 2000), for the expression of the flow rate, it is needed a secant linearization because the expression is at a vertical tangent at the linearization point, so it is possible to cover a significant range of pressure drops. By doing so, the linearized airflow rate equation is given by:

$$p_1 - p_2 = \dot{m} \cdot R_f \quad [35]$$

R_f is a parameter that defines a linear resistance to the flow and it was used by (Quaglia & Sorli, 2001) and (Robinson, 2012) to represent something similar to a damping coefficient. The representation of R_f was different in their researches because it depends on the flow resistance modelling and as the model considered in this model was the same of [Quaglia2], the expression of R_f adopted will be the following:

$$R_f = \frac{1 - b^*}{\rho_{atm} \cdot C} \quad [36]$$

Where $b < b^* < 1$ and its value will depend on the amplitude of the pressure oscillations around the linearization point.

Equations [30], [31], [34] and [36] describe the linearized air spring model.

2.5.2.1 Stiffness

By using the linear model, (Quaglia & Sorli, 2001) showed that is possible to analyze the stiffness of the system composed by just the spring or by spring plus reservoir around the operation point. Therefore, in this section, it will be demonstrated how the stiffness can change and how it affects the natural frequency of the system.

Firstly, the spring alone will be analyzed, i.e. the valve will be considered completely closed what, in the linear model case, means that $R_f \rightarrow \infty$ and consequently $\dot{m} = 0$. With these considerations, equation [30] becomes:

$$\dot{p}_1 = -\frac{np_{10}v}{V_{10}}\dot{h} \quad [37]$$

And so, equation [31] can be written as:

$$\dot{F} = -\frac{np_{10}vA_0}{V_{10}}\dot{h} + (p_{10} - p_{atm})\alpha\dot{h} = -\left(\frac{np_{10}vA_0}{V_{10}} - (p_{10} - p_{atm})\alpha\right)\dot{h} \quad [38]$$

By making a comparison between equations [8] and [31], we can notice that the term that multiplies \dot{h} in equation [31] is $K_S = K_{V1} + K_A$ and it depends on the volume variation and area variation. Therefore, each of the components of the stiffness can be written as:

$$K_{V1} = \frac{np_{10}vA_0}{V_{10}} \quad [39]$$

$$K_A = -(p_{10} - p_{atm})\alpha \quad [40]$$

K_{V1} is the volumetric stiffness and K_A is the area stiffness and both depends on the spring height variation. It is interesting to notice that depending of the air spring

shape one can have different values of stiffness, for example, for a rolling lobe spring in which the effective area variation is low, the value of K_A may be close to zero.

Now, to demonstrate a change in the system stiffness we consider a fully opened valve case, i.e. $R_f \rightarrow 0$ and we may assume that the system behaves as a spring with a volume equals to $V_{10} + V_{20}$. Then from equation [36] we have the pressure drop equals to zero (i.e. $p_1 = p_2$). By considering the last assumption and the equation [34] we have the following expression:

$$\dot{p}_1 = \dot{p}_2 = \frac{nRT_{20}}{V_{20}} \dot{m} \quad [41]$$

By replacing the last expression in equation [37] and by rearranging the terms, we have:

$$\dot{p}_1 = - \left(\frac{np_{10}v}{V_{10} + V_{20}} \right) \dot{h} \quad [42]$$

Analogously to the spring alone case, we replace the previous equation on [38], then we can write the stiffness as:

$$K_{SV} = K_{V12} + K_A = \frac{np_{10}vA_0}{V_{10} + V_{20}} - (p_{10} - p_{atm})\alpha \quad [43]$$

With the system stiffness defined we can do a quarter car model natural frequency analysis to understand that the opening and closure of the valve can change this system property. The following lines present a quarter car linear model natural frequency calculation for the cases of spring and spring plus reservoir.

- Spring:

$$\omega_S = \sqrt{\frac{K_{V1} + K_A}{M}} ; f_S = \frac{\omega_S}{2\pi} \quad [44]$$

- Spring + Reservoir:

$$\omega_{SV} = \sqrt{\frac{K_{V12} + K_A}{M}} ; f_{SV} = \frac{\omega_{SV}}{2\pi} \quad [45]$$

As $K_{V1} > K_{V12}$, then $f_S > f_{SV}$, what means that when the valve is being opened the system natural frequency is increasing and it does so until the valve is fully opened, as it will be explained better latter with the system frequency response analysis.

2.5.2.2 Transfer Functions

[Quaglia2] defines the pneumatic capacity as “the ratio of the mass flow rate entering or leaving a volume to the pressure gradient” and it is expressed by:

$$C_i = \frac{V_{i0}}{nRT_{i0}}, \quad i = 1, 2 \quad [46]$$

This notation will be used for a matter of simplification that will make it easier to write the transfer functions of the system.

From the linear equations [30], [31], [34] and [35] and from the equation [46], one can obtain the transfer functions of the system by applying the Laplace transform, what is crucial in the frequency response analysis and also is useful in a future control system implementation. Therefore, the transfer function between spring height h and spring force F is given by:

$$\frac{\bar{F}}{\bar{h}} = -K_{SV} \cdot \frac{sR_f C_2 \frac{K_{V12}}{K_{V1}} \left(\frac{K_S}{K_{SV}} \right) + 1}{sR_f C_2 \frac{K_{V12}}{K_{V1}} + 1} \quad [47]$$

The previous equation gives the relation between the spring deflection and the obtained force. However, an important characteristic to analyze is the relative displacement between the sprung and the unsprung mass, which is given by:

$$h = h_0 + (z - x) \quad [48]$$

By applying the Laplace transform in equation [48] and by substituting it on equation [47] we obtain the transfer function between excitation x and response z of the system.

$$\frac{\bar{z}}{\bar{x}} = \frac{sR_f C_2 \frac{K_{V12}}{K_{V1}} \left(\frac{K_S}{K_{SV}} \right) + 1}{s^3 R_f C_2 \frac{K_{V12}}{K_{V1}} \frac{m}{K_{V12} + K_A} + s^2 \frac{m}{K_{V12} + K_A} + s^2 R_f C_2 \frac{K_{V12}}{K_{V1}} \left(\frac{K_S}{K_{SV}} \right) + 1} \quad [49]$$

The previous mathematical model which was presented by (Cavanaugh, 1961) and deeper explored by (Quaglia & Sorli, 2001) is based on the approximation of a polytropic transformation of the air. According to (Moran & Shapiro, 2006), this process is valid for a closed system, therefore, when just the spring is considered the hypothesis is valid, however, when the mass of air inside the spring varies by the addition of the reservoir, the system considered is opened and the previous hypothesis becomes not so accurate. Even so, this model was validated with experimental tests, thus this thesis will be based on the analysis and the study of the air spring by exploring this model.

2.6 Control valve

The valve that is controlled in order to allow the passage of air between the air tank and the air spring was considered as a four-way valve. The valve model was

based on the idea presented by (Richer & Hurmuzlu, 2000) and the pneumatic system is illustrated by Figure 28.

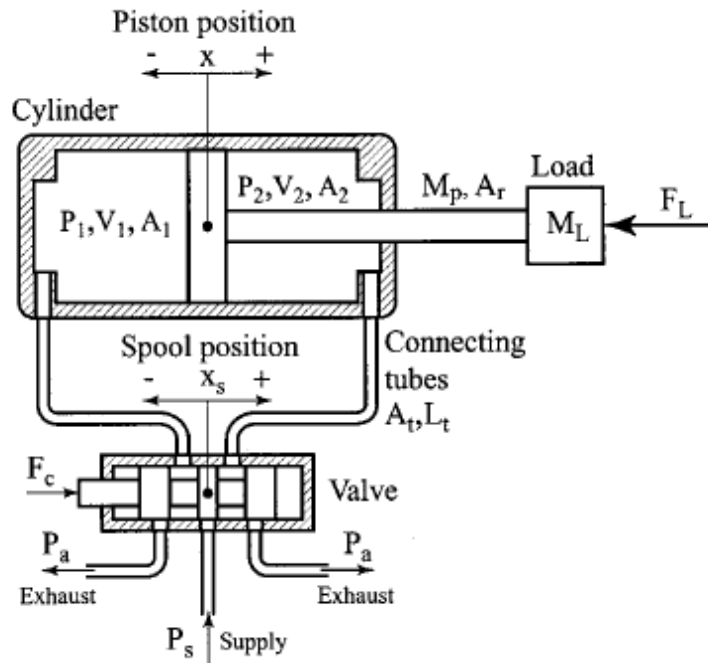


Figure 28 – Pneumatic system illustration (Richer & Hurmuzlu, 2000)

The pneumatic actuator proposed above actuates in two directions while the air spring that this project is based is only in one direction, so in section 3 it will be explained how it was adapted for this project.

The system includes a force element (pneumatic cylinder), a command device (control valve), connecting tubes and sensors. The working principle is simple: depending on the position of the spool that is activated by F_c , the valve is opened or closed. The valve model considered is shown by Figure 29.

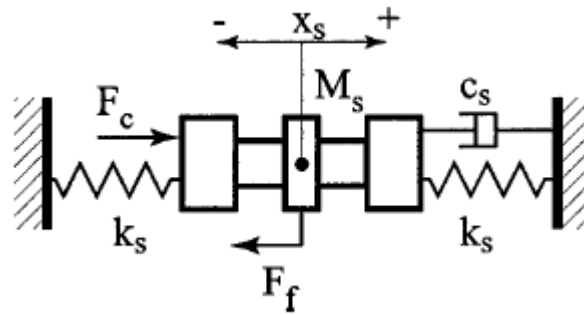


Figure 29 - Valve dynamic model (Richer & Hurmuzlu, 2000)

The model is a proportional valve which present some advantages as quasi-linear flow characteristic, small time constant, small internal leakage, ability to adjust both chamber pressures using one control signal, very low hysteresis, and low internal friction (Richer & Hurmuzlu, 2000). The spool equation of motion is given by:

$$M_s \ddot{x}_s = -c_s \dot{x}_s - F_f + k_s(x_{s0} - x_s) - k_s(x_{s0} + x_s)F_c \quad [50]$$

Where:

- M_s is the spool and coil assembly mass;
- x_s is the spool displacement;
- x_{s0} is the spring compression at the equilibrium position;
- c_s is the viscous friction coefficient;
- F_f is the Coulomb friction force;
- k_s is the spool springs constant;
- F_c is the force produced by the coil.

Considering that the friction force is negligible, and that $F_c = K_{fc}i_c$, where K_{fc} is the coil force coefficient and i_c is the coil current, one can rewrite the equation as:

$$M_s \ddot{x}_s + c_s \dot{x}_s + 2k_s x_s = K_{fc} i_c \quad [51]$$

Equation [51] gives the relation between the valve position and the input current in the system that will be used as a control parameter. Now, it is necessary to relate

the valve position with the orifice area, so we can calculate the airflow rate later. Figure 30 illustrate the valve spool and the orifice area working principle.

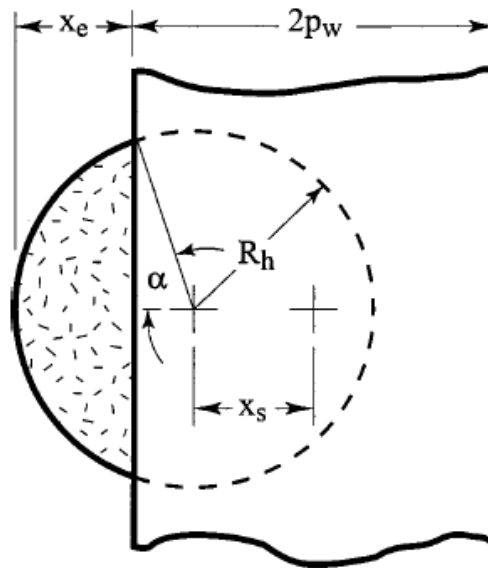


Figure 30 - Valve orifice and spool displacement (Richer & Hurmuzlu, 2000)

It is important to highlight that, for this model of proportional valve, when the spool moves to a specified limit position, the valve opens the inlet orifice and closes the outlet orifice, what guarantees the air spring inflation. However, when the spool moves to the opposite limit position, the valve closes the inlet and opens the outlet orifices, what causes the air spring to deflate. The equations that give the valve effective area for inlet and outlet paths are:

$$A_{v_{in}} = \begin{cases} 0 & \text{if } x_s \leq p_w - R_h \\ n_h \left[2R_h^2 \arctan \left(\frac{R_h - p_w + x_s}{R_h + p_w - x_s} \right) - (p_w - x_s) \sqrt{R_h^2 - (p_w - x_s)^2} \right]^* & \text{if } p_w - R_h < x_s < p_w + R_h \\ \pi n_h R_h^2 & \text{if } x_s \geq p_w + R_h \end{cases} \quad [52]$$

* if $p_w - R_h < x_s < p_w + R_h$

$$A_{v_{ex}} = \begin{cases} \pi n_h R_h^2 & \text{if } x_s \leq -p_w - R_h \\ n_h \left[2R_h^2 \arctan \left(\sqrt{\frac{R_h - p_w + |x_s|}{R_h + p_w - |x_s|}} \right) - (p_w - |x_s|) \sqrt{R_h^2 - (p_w - |x_s|)^2} \right] & \text{if } -p_w - R_h < x_s < R_h - p_w \\ 0 & \text{if } x_s \geq R_h - p_w \end{cases} \quad [53]$$

* if $-p_w - R_h < x_s < R_h - p_w$

Where:

- $x_e = x_s - (p_w - R_h)$ is the effective displacement of the valve spool;
- R_h is the orifice radius;
- p_w is the half of spool width;
- n_h number of active holes for an air path

According to (Ben-Dov & Salculean, 1995), the valve flow is given by the following equation:

$$\dot{m}_v = \begin{cases} C_f A_v C_1 \frac{P_u}{\sqrt{T}} & \text{if } \frac{P_d}{P_u} \leq P_{cr} \\ C_f A_v C_2 \frac{P_u}{\sqrt{T}} \left(\frac{P_d}{P_u} \right)^{\frac{1}{k}} \sqrt{1 - \left(\frac{P_d}{P_u} \right)^{\frac{k-1}{k}}} & \text{if } \frac{P_d}{P_u} > P_{cr} \end{cases} \quad [54]$$

Where:

- C_f is a nondimensional discharge coefficient;
- P_u is the upstream pressure;
- P_d is the downstream pressure;
- $P_{cr} = \left(\frac{2}{k+1} \right)^{\frac{k}{k-1}}$ is the critical pressure ratio;
- $C_1 = \sqrt{\frac{k}{R} \left(\frac{2}{k+1} \right)^{\frac{k+1}{k-1}}}$;
- $C_2 = \sqrt{\frac{2k}{R(k+1)}}$.

By substituting equations [52] and [53] into equation [54] we can calculate the airflow through the valve. This is a nonlinear model that will be adapted for this project in order to use in a first approach control system and it will be discussed in the next section.

This concludes all the literature review that supports this thesis and in the next section the methodology used will be presented, so it will explain the steps taken and the adaptations and implementations needed to do all the required simulations. Later obtained results will be discussed, what includes the analysis of availability of the pneumatic system for a small city car.

3 Methodology

Aiming to design an air spring to a city car, there are some projects constraints, for example, space and pressure restrictions, that will be considered in order to reach the optimum design. In this section it will be explained the methodology used to analyse and study the design of an air spring and some dynamic characteristics that can be controlled to help the comfort improvement so reaching a design that fills the project requirements.

This section is basically divided in four parts. The first one includes how the model presented in the last section was explored and adapted, thus it is composed by a brief explanation of the Simulink with the block diagram logics and the hypothesis utilized.

The second part includes the steps followed to design the air spring as well as the parameters explored, then it will be presented the values for a comparison with the literature results, i.e. the model validation.

In the third part it will be presented some values that will be used to study the effects of the design parameters in the spring dynamic behaviour. After understanding these effects, some values will be proposed in order to optimize the air spring characteristics for a city car and in the end some air springs already existing on the market will be suggested to fit on the desired behaviour and desired project requirements.

The last part includes the air spring plus auxiliary reservoir model as well as a model that includes the pressurized tank that will be used to study the filling ratio of the spring, i.e. an analysis of the time required to fill up the spring until the desired pressure is reached.

3.1 Model implementation

The model was implemented in MATLAB-Simulink as shown in Figure 31 - Simulink block diagram.

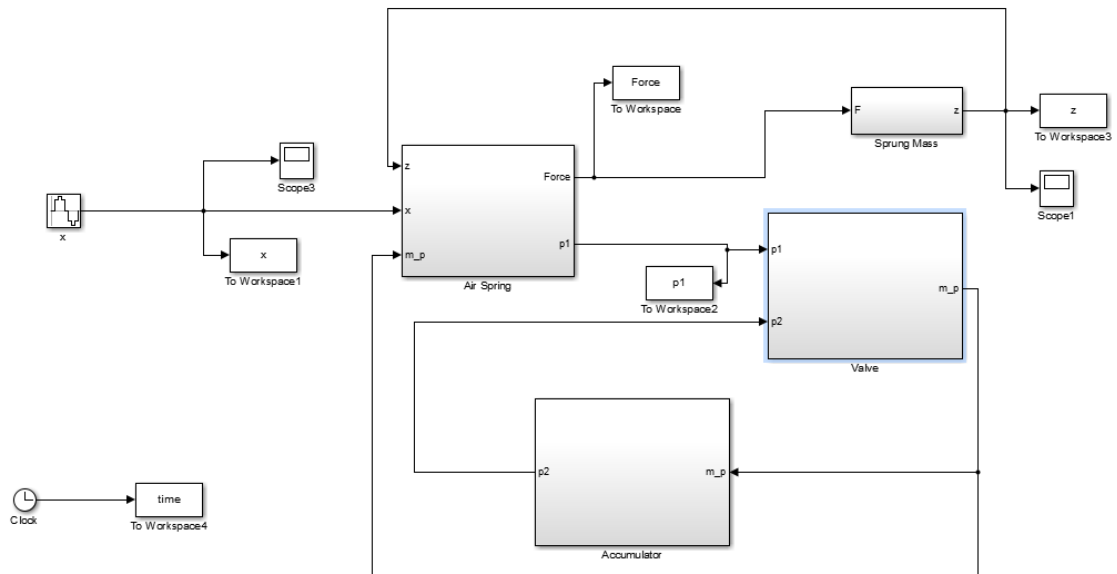


Figure 31 - Simulink block diagram

In this figure it is shown the sinusoidal input, however the input was changed according to the desired simulation. The solver was the ode3 with fixed-step size of 0.001. There are integrations and derivations in continuous and in discrete mode that were used in order to avoid initial undesired peaks generated by the solver might compromise the simulation results.

To simplify the model some assumptions were made, they are:

- Air is considered an ideal gas;
- The system is considered thermally isolated, so the process is assumed as adiabatic;
- Friction forces are considered negligible;
- Elastic properties of the rubber are considered negligible;

The logic of the diagram begins with a road profile input that will give the position of the bottom part of the spring (x), as the model works with just one degree of freedom. The input goes to the Air Spring block where the displacement x is converted to spring height variation, i.e. relative displacement between bottom and top part of the spring ($h = z - x$). Equations (18) and (21) are used in this block so the spring pressure p_1 and spring force F can be calculated. While the force is used on the sprung mass block to calculate the displacement z , p_1 , together with p_2 , is used to calculate the airflow

rate (\dot{m}) in the valve block by using the equation (23). Now, with equation (24), \dot{m} is used to calculate the auxiliary reservoir pressure p_2 , that is used as feedback to the valve block, and as an input of air spring block to compute p_1 .

3.2 Model Validation

Values of spring volume and area were taken from (Quaglia & Sorli, 2001) for validation proposes and they are given by Figure 32.

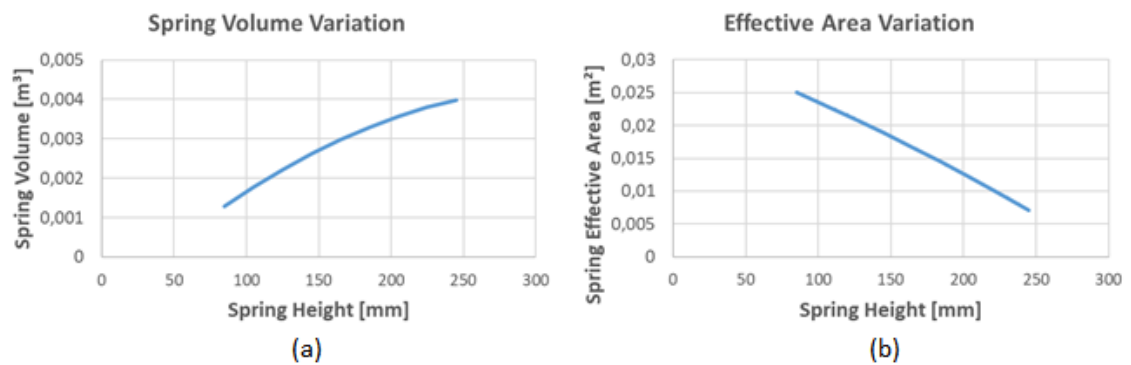


Figure 32 - Reference spring (a) volume and (b) effective area variation

From the volume and effective area curves, it was possible to approximate them by the following second order polynomial equations:

$$V_1(h) = -0.0549 h^2 + 0.035 h - 0.0013 \quad [55]$$

$$A_{eff}(h) = -0.0942 h^2 - 0.0811 h + 0.0326 \quad [56]$$

The spring that is used as reference to validate the model is the same that was used by (Quaglia & Sorli, 2001): a T26 double bellows spring from Pirelli. The data is given by Table 1.

Table 1 - Spring and Simulation Data

Initial Spring Height (h_0)	165 mm
Sprung Mass (M)	285 kg
Initial Spring Volume (V_{10})	0.00298 m ³
Effective Area (A_{eff})	0.01667 m ²
Auxiliary Volume (V_2)	0.012 m ³
Initial Spring Pressure (p_0)	2.682 Bar
Environment Pressure (p_{atm})	1.01 Bar
Environment Temperature (T_{env})	283.15 K
Gravitational Acceleration (g)	9.78 m/s ²
Air Ideal Constant (R)	287 J/kg.K
Specific Heat at Constant Pressure (c_p)	1.005 J/kg.K
Specific Heat at Constant Volume (c_v)	0.718 J/kg.K
Pressure Ratio at Laminar Flow (β_{lam})	0.999
Critical Pressure Ratio (b)	0.528
Environment Air Specific Mass (ρ_{atm})	1.185 kg/m ³

With the equations (18), (21), (23) and (24) in the block diagram and the data from Table 1, it is possible to do the simulations of the nonlinear model. The simulation involves the whole system spring and reservoir subjected to a step input with two values of amplitude (2 mm and 10 mm) and the opening and closure of the valve is controlled by giving the values the sonic conductance. In the simulation in question, three values of conductance were used as input variables: $C_1 = 0.5 * 10^{-9}$, $C_2 = 10 * 10^{-9}$ and $C_3 = 20 * 10^{-9}$. The results were compared to the literature's and discussed in section 4.

For the linear model validation, equations (16), (47) and (49) were used together with data from Table 1. Moreover, the linear volume and area variations need to be determined and their values are given by:

$$v = \left. \frac{dV}{dh} \right|_{h_0} = 0.0169 \quad [57]$$

$$\alpha = \left. \frac{dA_{eff}}{dh} \right|_{h_0} = -0.1122 \quad [58]$$

By using the Bode plot function of MATLAB in equations (47) and (49) it was possible to simulate a frequency response of the system for the transmissibility of the force and the relative displacement between sprung mass and wheel. The results are compared and discussed in section 4.

After validating the model by comparing solutions with the literature, it is ready to be explored and to test other types of springs with different characteristics, so it is possible to analyse some solutions for the small city car project requirements.

3.3 Design Parameters

With the working model, it is possible to study the spring pressure, stiffness and force during compression and extension. The simulations involved will give as results the characteristics of the reference spring and they represent the behaviour of an air spring, therefore they will be used as characteristics curves of the spring.

As already said, spring volume and effective area variation rule the spring dynamic behaviour, so they will be the main design parameters. It is important to see how each one of them affects the spring characteristics and what could be the values to achieve the project requirements.

In order to do this analysis, firstly the volume effects are studied and then the effective area ones separately. Therefore, three springs with different volume variations but the same effective area are proposed to be compared to the reference one, where these values are represented in Figure 47. Analogously, another simulation is done but with a fixed volume and different effective areas instead and the values are shown in Figure 50. It is important to point out that, in this volume and effective area study, the relation between them is not considered, they were considered independent parameters in an ideal situation just to see how each of them interferes on the spring characteristics. However, usually they are related, for example, bigger air springs have

higher volumes and higher effective areas while smaller ones have the opposite characteristics.

As we know how the previous parameters affect the spring behaviour, we can focus on the project requirements for a small city car to choose a final design for the air spring. In this case, the air spring must be as most compact as possible and support the maximum dynamic loads required.

3.4 Air spring and auxiliary reservoir

By adding an auxiliary reservoir there is the inclusion of a valve that connects the it to the air spring. By including this valve, it is possible to obtain a damping for the system, however, it brings also a hysteresis effect that is important in the final spring force calculation.

The model is the same used in the design parameters analysis, but the sonic conductance C is changed by increasing the diameter of the valve.

3.5 Air Tank

The model with the auxiliary reservoir was adapted to include an air tank instead of an accumulator. By doing so, one can study the time needed for the spring to reach the desired force. Figure 33 shows the new system model including an air tank.

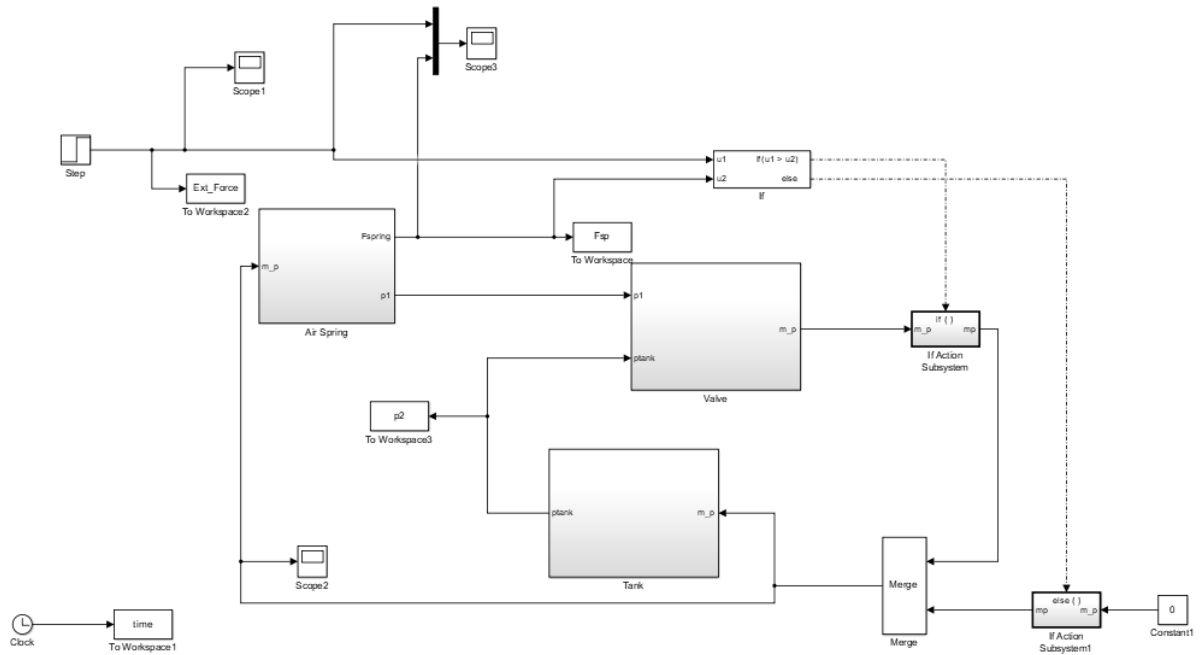


Figure 33 - Spring and air tank model

This model adapts the auxiliary reservoir as an air tank, and it considers the same valve model as before, i.e., the same equations are applied in each subsystem. By doing so, a valve diameter was selected only to demonstrate the effects of fulling the air spring and draining the air tank.

The data used for the air tank was based on the most common models found in the market. Table 2 shows the tank data used on the simulations.

Table 2 - Air Tank Data

Tank	Pressure (Bar)	Volume (L)
1	13.79	1.89
2		3.78
3		7.57
4	10.34	1.89
5		3.78
6		7.57

This simulation considers a situation in which a specific spring force is required, as it can happen when the vehicle is doing a curve and it is submitted to a roll case. Thus, a force was estimated as 4.7 kN and considered as a step input in the system.

With the valve opened, it was calculated the time needed to fulfil the air spring accordingly to the tank volume and pressure. Also, it was possible to calculate the tank final pressure which is important in the case we have many forces inputs what implies that the tank can be quickly drained.

Another configuration simulated was the model with a compressor that fulfil the air tank when it is drained. By using the data of an already existing model of compressor (444C Viair), it was possible to study the time needed to fulfil the air tank after a certain pressure demand was taken. Figure 34 shows the configuration with the compressor.

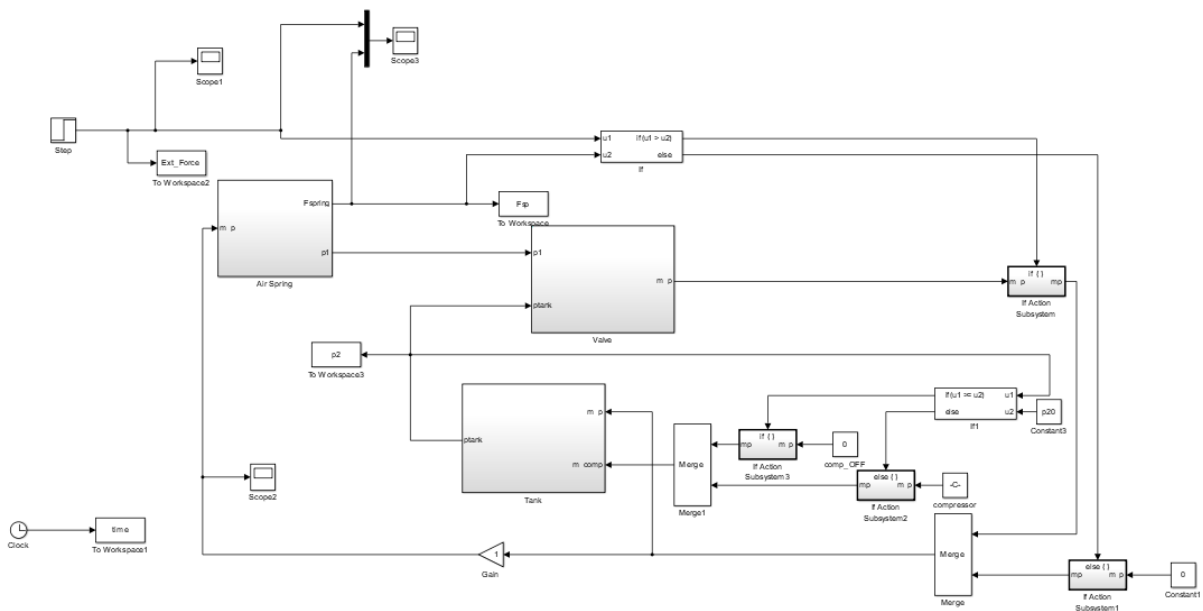


Figure 34 - Air tank model with compressor

Again, in this model, a required force is modelled as a step input and with the opened valve the air spring is fulfilled by the air tank. At the same time, when the air tank pressure starts to decrease the compressor turns on and begins to fulfill the air tank.

3.6 Control System

After the air spring is modeled, as well as the airflow and the air tank, we need a control strategy in order to have an active system. As explained in section 2.6, we are using a proportional valve and it was modeled in Simulink as illustrated by Figure 35.

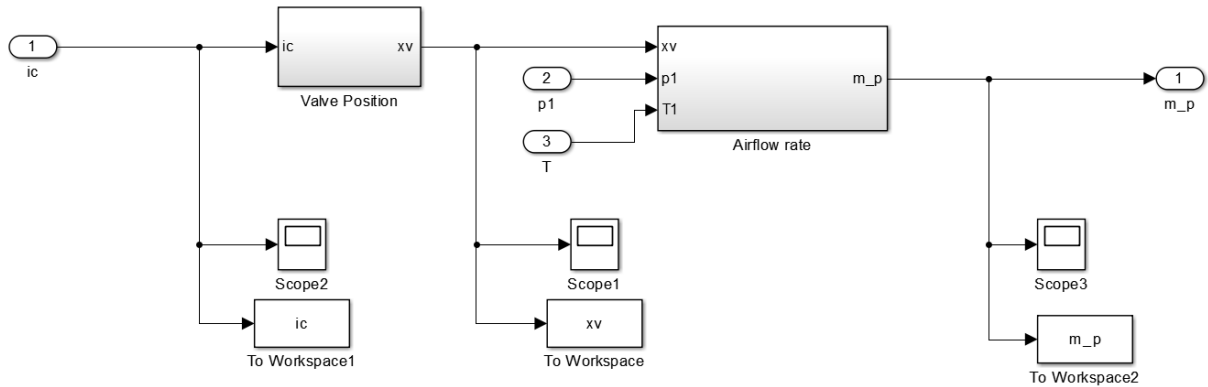


Figure 35 - Valve model Simulink

Inside the block “Valve Position” we implemented equation [51] and inside the block “Airflow rate” we implemented equations [52], [53] and [54]. The data used for modeling the valve is expressed by Table 3.

Table 3 - Proportional valve data

Valve Data	
k	1.4
C_f	0.25
k_s	80 N/m
c_s	7.5 kg/s
K_{fc}	2.78 N/A
n_h	1
p_w	3.1 mm
R_h	3 mm

For a first approach of a control strategy, a model without the valve was implemented with the quarter car model to analyze the effects of the actuator in the system as illustrated by Figure 36. For the controller, a simple PID block was implemented and the gains were calculated by MATLAB “Tune” option, since the goal is just to verify the availability of the system.

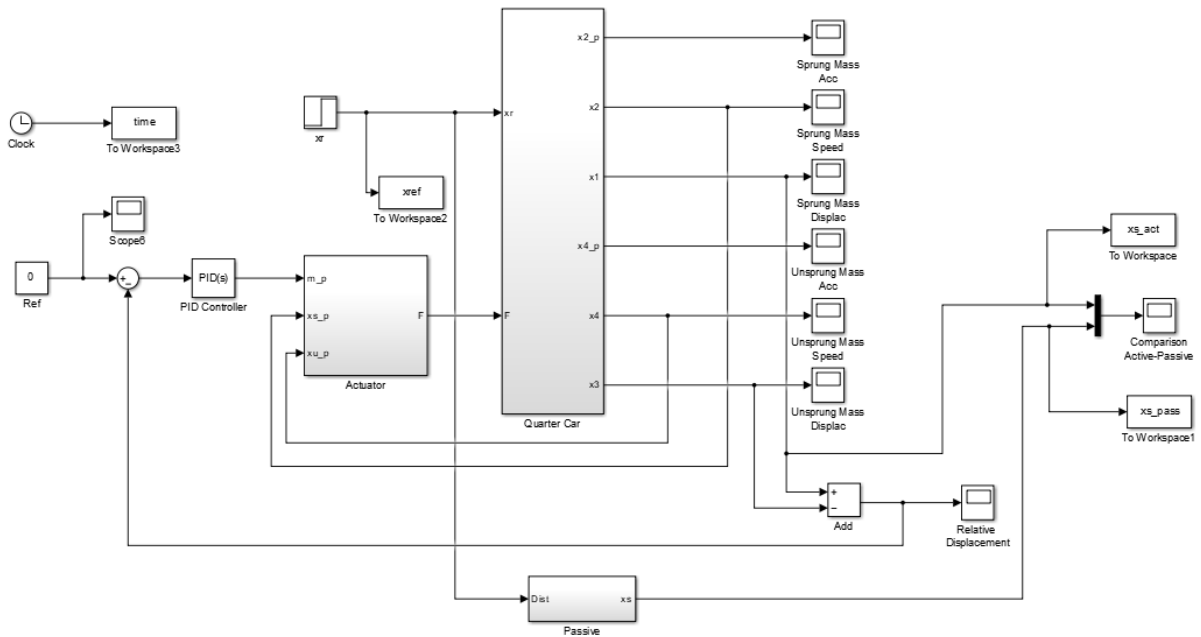


Figure 36 - Active configuration without control valve

The model above illustrates the quarter car active configuration without the control valve, so, in this case, the PID controller is actuating on the mass air rate that fills the air spring.

For a full configuration including the proportional valve, a second model was developed, and it is illustrated by Figure 37.

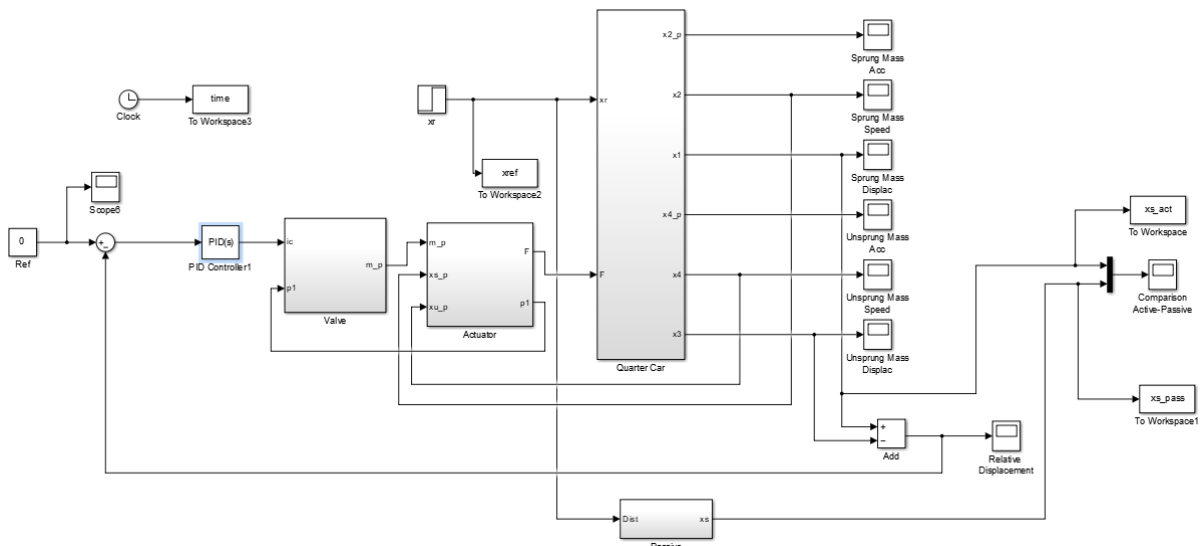


Figure 37 - Active configuration with valve

One can see that in this new model the PID controller is actuating on the proportional valve, and it is controlling the coil current of the valve spool as it happens in the real model.

Besides the valve nonlinear model works fine alone, when implemented to the quarter car model it caused some errors on MATLAB derivative algorithm, thus to solve this issue some equations were linearized to simplify the calculations. As the focus of this project is just to verify the availability of the pneumatic system in a small city car, this solution was considered reasonable even because this is just a first approach of the control system, so other control strategies must be tested to guarantee the optimum solution and could be the focus of future works.

4 Results and discussion

In this section the simulation results will be analysed and discussed. Firstly, the model validation results will be presented and after that the effects of the design parameters will be explained, as well as how they can be changed in order to reach a desired dynamic behaviour according to the project requirements. In the end, some results about the first approach control strategy will be discussed.

4.1 Validation Results

In the previous section, it was explained that two models were used for the validation: the nonlinear and the linear. Firstly, the nonlinear model will be compared and discussed.

Figure 38 shows the results of (Quaglia & Sorli, 2001) model for a step response using the nonlinear model while Figure 39 shows the same simulation for the implemented model of this thesis.

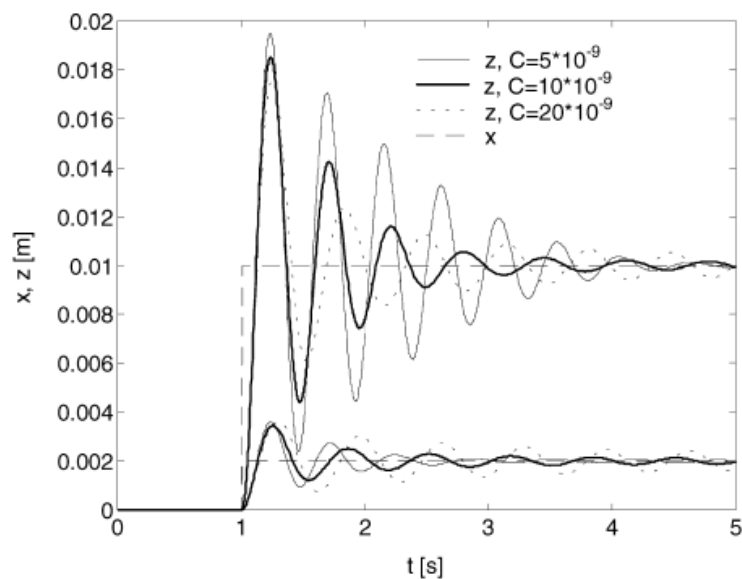


Figure 38 - Nonlinear model step response $[C] = \text{m}^3 / (\text{s} \cdot \text{Pa})$ (Quaglia & Sorli, 2001)

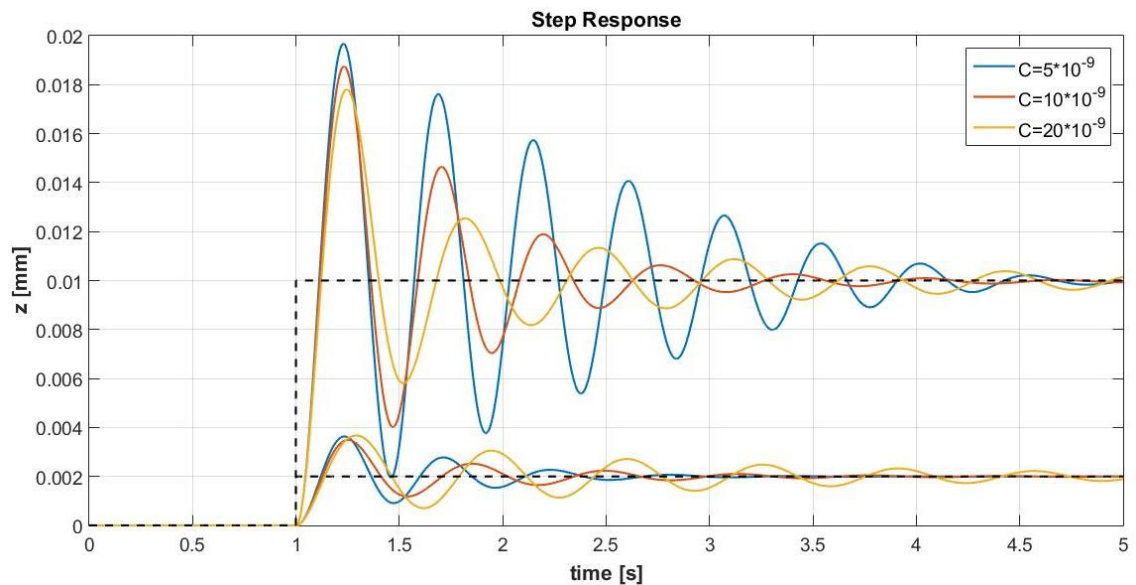


Figure 39 - Implemented nonlinear model step response [C] = $m^3/(s \cdot Pa)$

According to the figures, the implemented model gave acceptable results, with a maximum error of 3%. It is possible to see that the based model is more damped than the implemented one and it is believed that the reason for that is the valve modelling, that could had been differently implemented. The valve modelling of this project was based on the three equations (laminar, subsonic and choked) presented on the ISO 6358 and by analysing Quaglia's work it can be noted that he uses just two of them. (24) indicates that the equation to be used for the airflow rate calculation depends on the ratio $\frac{p_o}{p_i}$, that was found to be close to 1 many times during a step response, however, in the reference literature this was not considered in his valve model.

The simulation involves a 10 mm step and three positions of the valve that produce three different conductances. By analysing the results, it is possible to note the difference in damping behaviour according to the valve orifice area, i.e., by opening the valve, the sonic conductance C is being increased and so the peak amplitudes change. It is important to note that when $C = 5 \cdot 10^{-9}$ the system has the largest initial peak and the oscillation attenuation is not so effective. When $C = 20 \cdot 10^{-9}$ the initial peak is the smallest, however the small oscillations tend to last more than the case with $C = 10 \cdot 10^{-9}$. Therefore, to efficiently control the oscillations, the control of the

valve should consider the amplitude of the oscillation, i.e., for the initial peak, the valve should be more opened ($C = 20 \cdot 10^{-9}$) to damp larger oscillations and then, when the oscillation peak is decreased the valve should close a little ($C = 10 \cdot 10^{-9}$) to damp smaller oscillations.

As told in section 3, the linear validation involves the frequency response and for this analysis two simulations were done: force transmissibility and relative displacement. Figure 40 presents the literature results for the first case and Figure 41, the obtained results to compare with them.

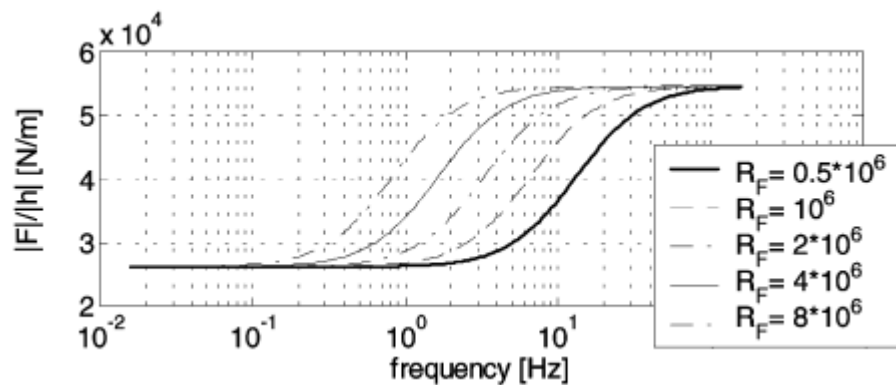


Figure 40 - Frequency Response - Force Transmissibility (Quaglia & Sorli, 2001)

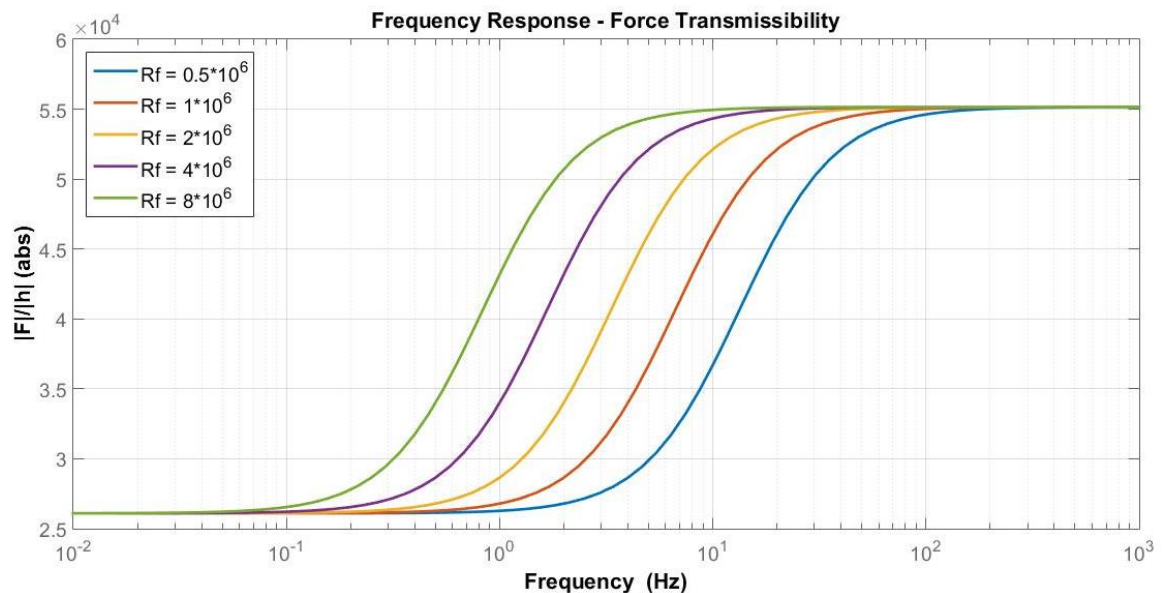


Figure 41 - Frequency Response – Force Transmissibility results

The obtained result is similar to the one provided by the literature, so the model for this simulation is working adequately. In the figures, it is possible to see when there is the phase changing and as the resistance is being changed so does the phase difference, what can be seen better in the next figures. Moreover, the phase difference between force and spring height is responsible for the damping effect and when the linear resistance (R_f) is changed, this effect is also changed, so it can be controlled to achieve an optimum damping.

The next lines are related to the second validation simulation for the linear system, i.e., the relative displacement frequency response. Figure 42 and Figure 43 show the linear system frequency response of the reference and the implemented models respectively.

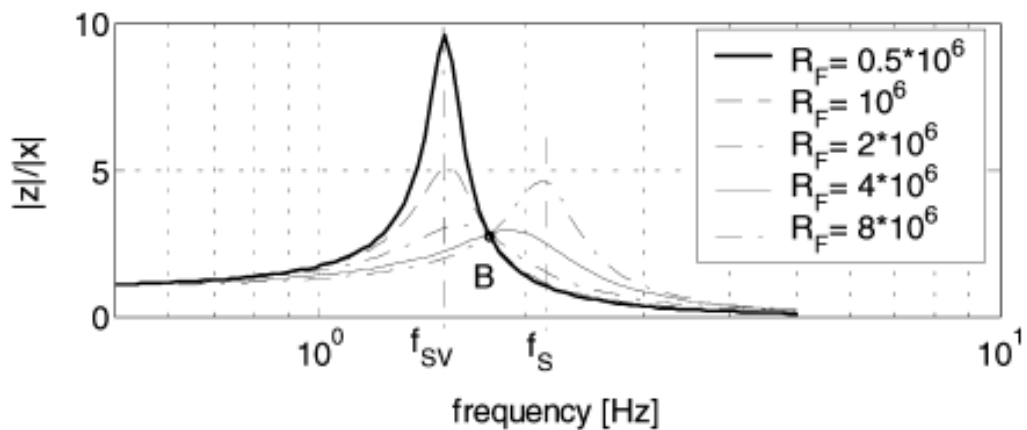


Figure 42 - Frequency response for the reference quarter-car model [R_f] = Pa/(kg/s) (Quaglia & Sorli, 2001)

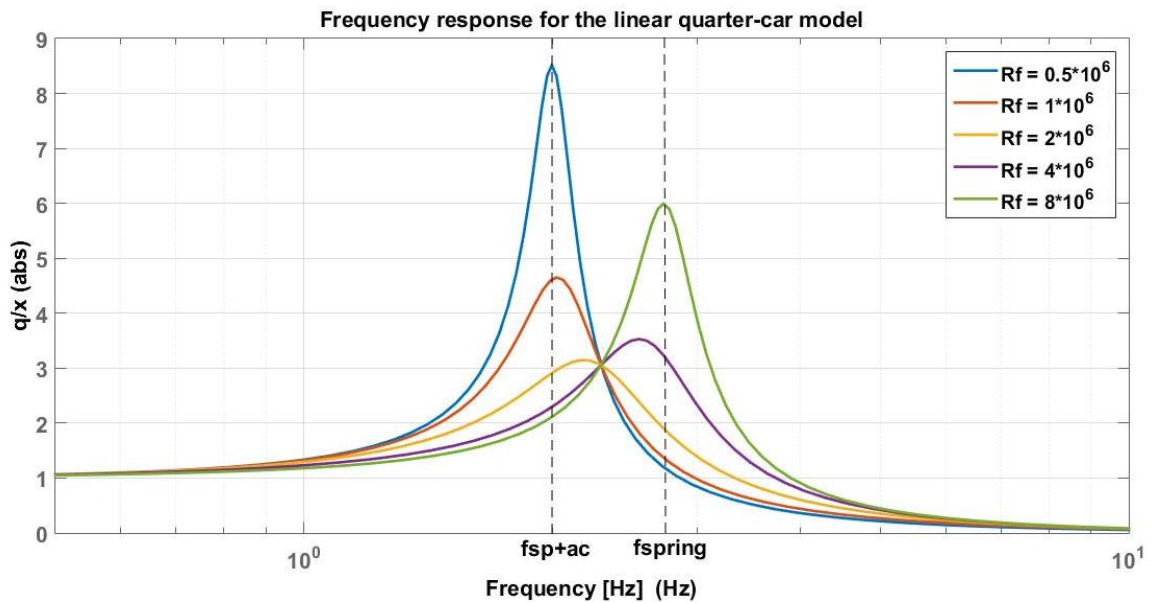


Figure 43 - Frequency response for the implemented quarter-car model [R_f] = Pa/(kg/s)

In this case the results were the same and then the implementation can be considered successful. As the linear model is being analysed, the conductance was replaced by the linear resistance coefficient R_f and the simulations include the variations of this parameter to simulate the closure or the opening of the valve.

As explained in section 2.5.2.1 the opening and closure of the valve can change the natural frequency of the system and this can be noted in the figure above. Then, when R_f is the lowest (valve considered opened) the natural frequency of the system is the lowest and when R_f is the largest (valve considered closed) the natural frequency of the system is the largest. It can be confirmed by using the data of Table 1 and the equations (44) and (45), that give:

$$f_{spring} = 2.214 \text{ Hz}$$

$$f_{sp+ac} = 1.523 \text{ Hz}$$

Then, together with the step response analysis, it is possible to see that by closing the valve the system becomes undamped, what can be explained by the fact that by closing the valve we are eliminating the factor responsible for the energy dissipation. Moreover, the system tends to be undamped when the valve is completely

opened because the pressure drop between main chamber and reservoir is eliminated and so there is no energy dissipation. In this last case, the total spring volume considered would be the volume of the spring plus the volume of the reservoir, and so the spring would be softer.

Also, it is interesting to note that all the R_f curves passes through the point B, therefore, the optimal resistance for the system is the one in which the maximum frequency occurs at this point. As the value of the intersection B is related to the maximum and minimum resistance curves, the design of the system should consider that the natural frequencies f_{sp+ac} and f_{spring} must be as far as possible, so the maximum peak of the optimal resistance (i.e. the maximum value of B) can be the lowest.

4.2 Pressure, force and stiffness analysis

With the proposed model and the data provided in section 3 it is possible to analyse the spring pressure, force and stiffness data. At the beginning, only the air spring alone is studied so it is possible to get the spring pressure and stiffness variation and after that the reservoir is added and its effects are analysed.

Figure 44 - Spring Pressure x Spring Height presents the spring pressure behaviour during a compression and extension cycle.

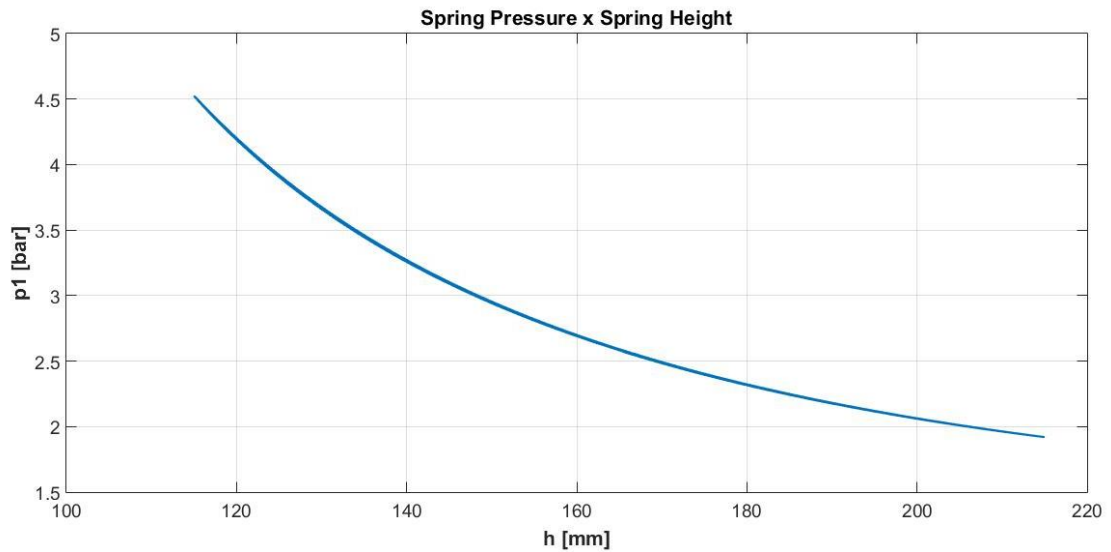


Figure 44 - Spring Pressure x Spring Height

The simulation was done considering a conductance so low that the airflow rate between spring and reservoir could be considered negligible, i.e., the valve is considered closed. The initial height of the spring is $h_0 = 165 \text{ mm}$, the input was sinusoidal with an amplitude of 50 mm and the sprung mass height was considered fixed, otherwise the values of the pressure would present a discontinuity point due to the shape of the curve that gives the sprung and unsprung mass relative displacement.

The previous figure shows that when the spring is compressed the pressure increase and when the spring is extended the pressure decrease, what was expected. Moreover, the curve presents some hysteresis effect due to the nonlinear behaviour and compressibility of air, that will be increased when opening the valve.

Now, following the same parameters for the pressure analysis, the spring stiffness behaviour is shown by Figure 45.

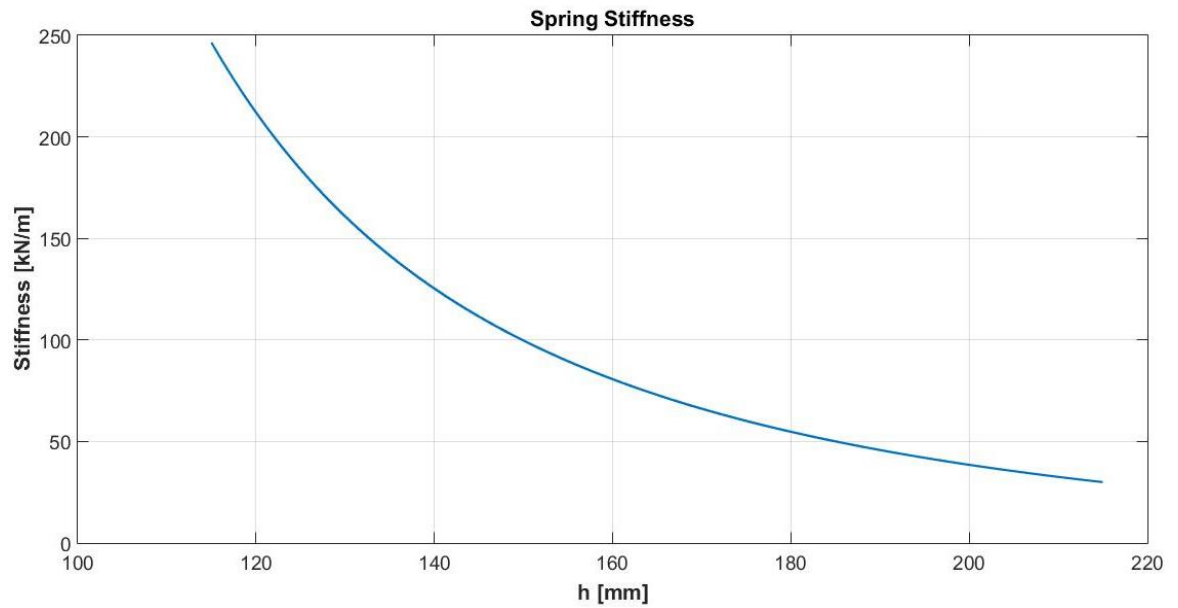


Figure 45 - Spring Stiffness x Spring Displacement

The curve shows an expected behaviour in which the stiffness increases when the spring is compressed and decreases when the spring is extended. This can be explained by the equation (39) in which the stiffness is proportional to the spring pressure and inversely proportional to spring volume. Then, when the spring is compressed, the spring volume decreases and the pressure increases, so it makes the stiffness to increase, and the opposite happens when the spring is extended.

Another obtained result is from the force calculation, that is done by integrating equation (21), and it is shown in Figure 46.

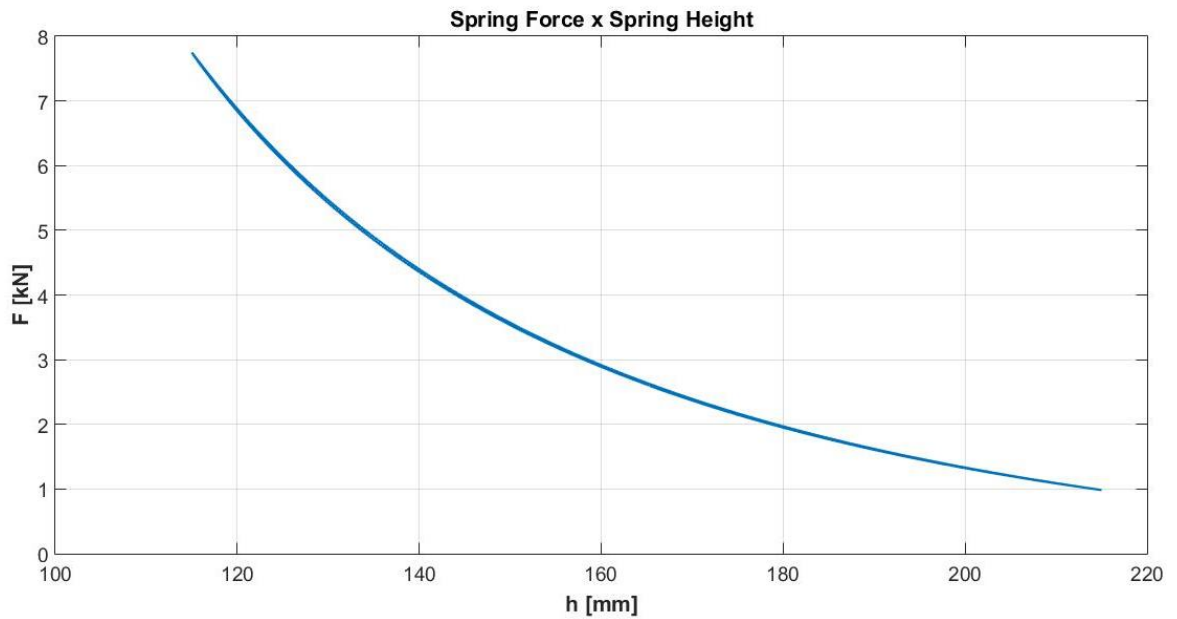


Figure 46 - Spring Force x Spring Height

As expected, the spring force increases when the spring is compressed and decreases when the spring is extended, proved by the equation (39) and the behaviour of stiffness curve. Also, the force presents the hysteresis characteristic what can be considered an issue and must be controlled.

The maximum calculated force was approximately 7.8 kN, which is enough when compared to an extreme case where the force required by a small city car under 2.5g acceleration is approximately 7.3 kN. Thus, this type of air spring can provide the required force, but if the spring force is not enough, some spring parameters must be changed, as it will be demonstrated in the next section.

4.3 Parameters analysis

The most important parameters when designing an air spring are the air spring volume and the air spring effective area. Some simulations results will be presented in this section and they consider different values of spring volume and area to compare the effects of these parameters.

4.3.1 Volume

Firstly, it is assumed an analysis of three springs with different volumes, presented in Figure 47, but the same effective area, so we have the effect of the spring volume on the spring force, as shown in Figure 48.

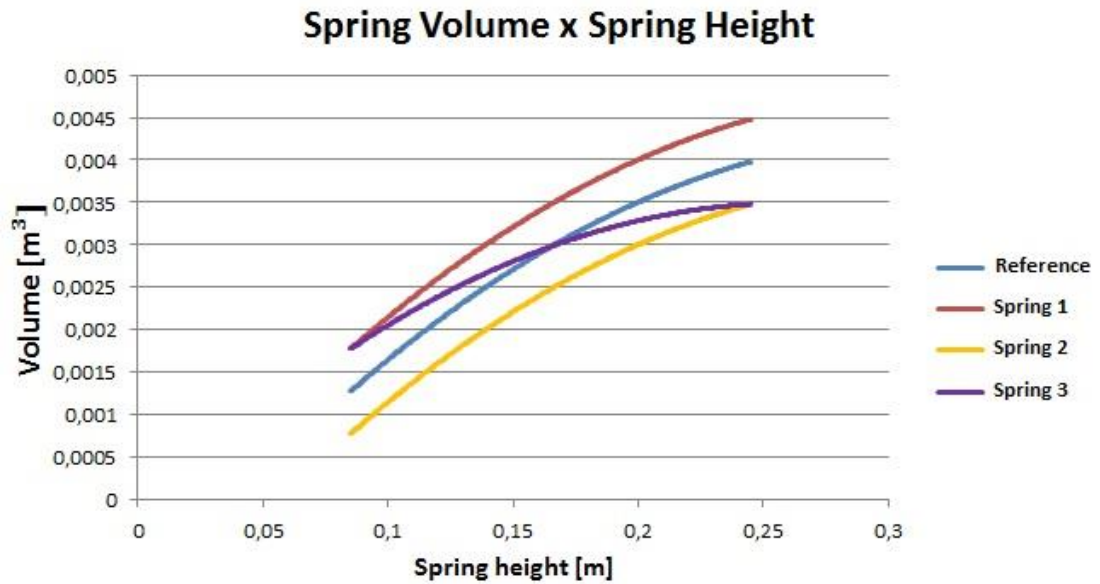


Figure 47 - Volume Variation Comparison

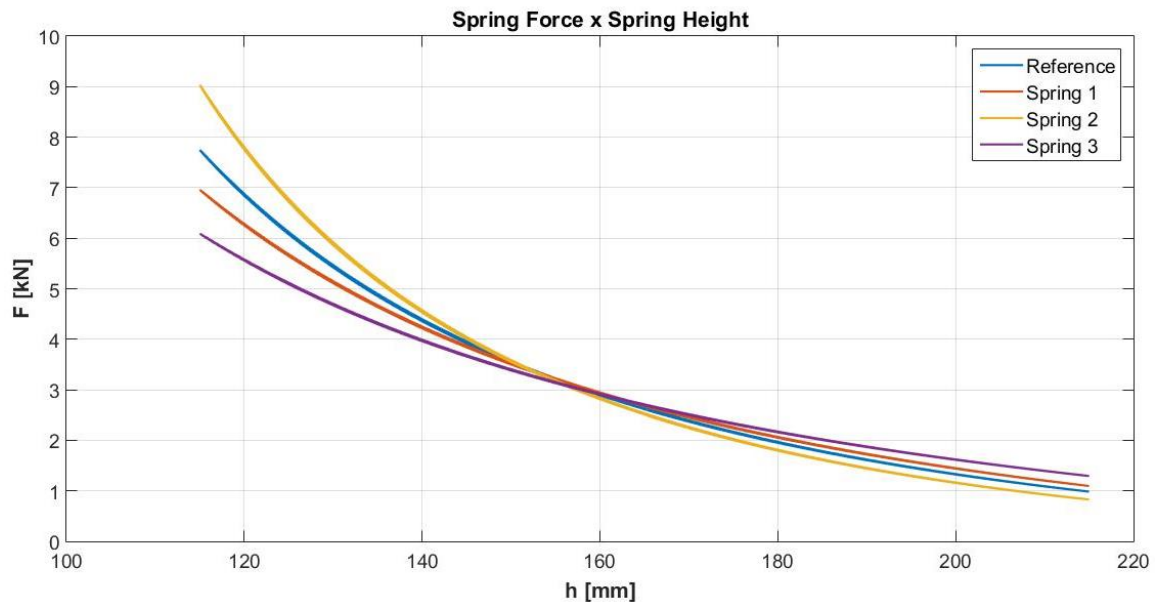


Figure 48 - Spring Force for different spring volumes

It is possible to see the volume affects the force behaviour. In this case were analysed three types of springs in comparison to the reference one, i.e., the spring used in Quaglia's work. The most visible difference is the force behaviour in compression in which the spring with the highest volume (spring 1) gives a lower force than the reference while the smallest spring (spring 2) gives the highest force. Spring 3 gives the lowest force, what is expected because, from Figure 47, we see that this spring has the lowest volume variation, what means that also the force variation will be lower. For the cases of springs 1 and 2, the force result can be explained by the spring pressure, that is higher for spring 2 than for spring 1 due to the volume difference, as shown by Figure 49.

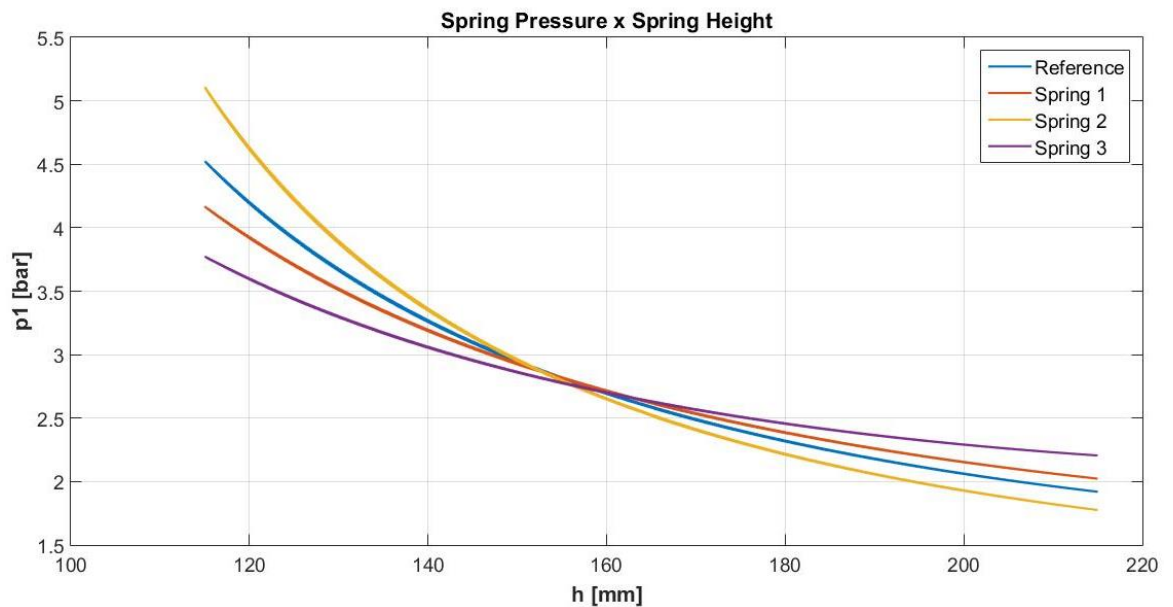


Figure 49 - Pressure variation according to different spring volumes

4.3.2 Effective Area

The next lines show the effective area variation and the analysis of what happens to force generated when we have a bigger area, or a smaller area compared to the reference. Figure 50 presents the area variation for three other types of springs and Figure 51 shows the variation in force.

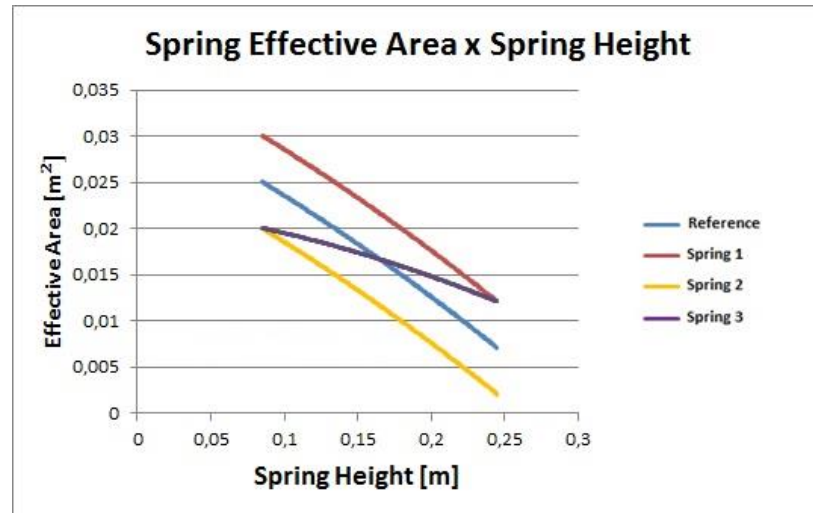


Figure 50 - Effective Area variation comparison

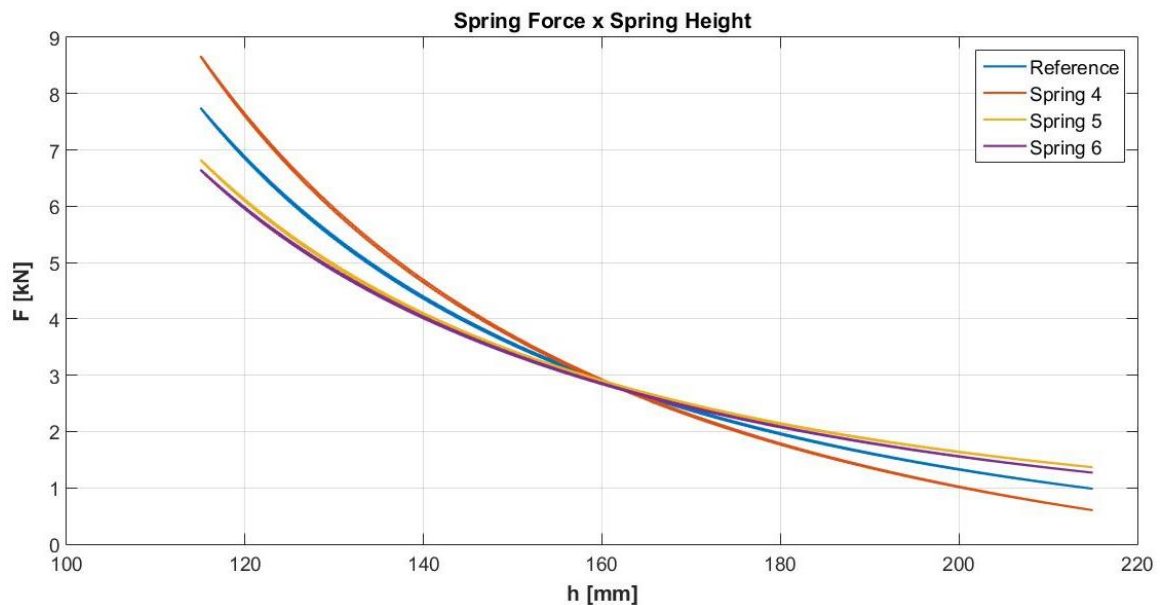


Figure 51 - Spring Force x Spring Height for different values of effective area

In the case of increasing the effective area of the spring we have an increase of the spring force during compression due to the proportionality relation between them, as shown in equation (6), but in extension the opposite occurs. Springs 5 and 6 generates similar forces what is interesting since their effective area variation is different and it shows the complexity and the need for experimental tests in air spring design. Also, it is important to highlight that, according to equation (18), the spring pressure does not depend on the effective area, therefore p_1 behaviour for these springs is represented by the pressure curve of reference spring, shown by Figure 44.

4.3.3 Rolling diaphragm spring

For this type of spring an assumption can be imposed: $K_A \cong 0$, i.e., the effective area variation is considered negligible. With this hypothesis the characteristics of the rolling diaphragm spring were analysed, and the results are shown by Figure 52 and Figure 53.

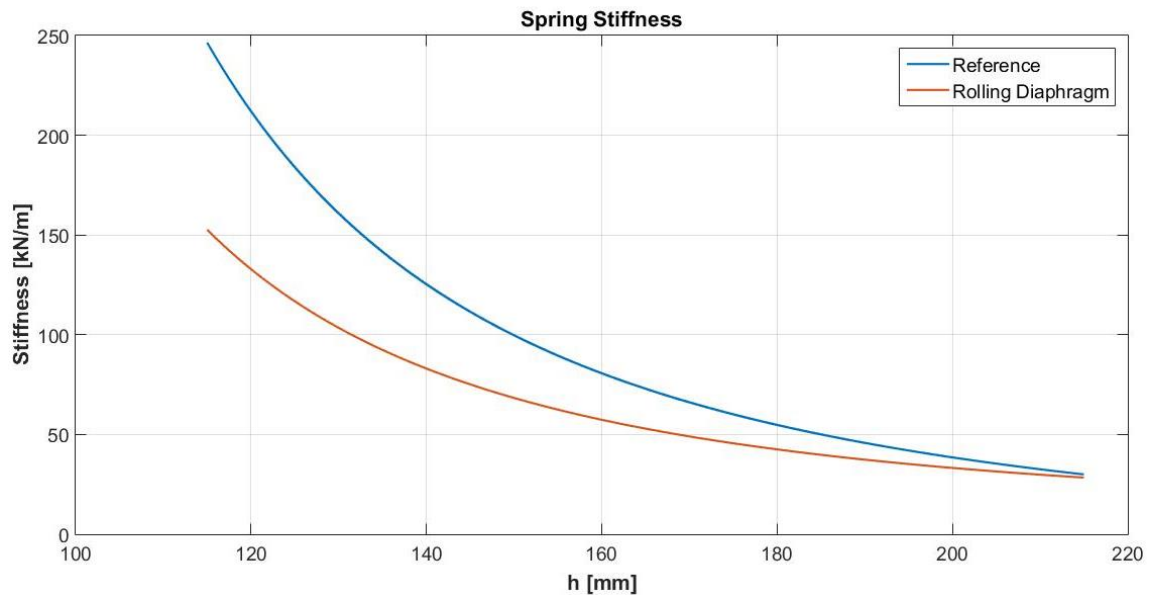


Figure 52 - Spring Stiffness x Spring Height for a rolling diaphragm spring

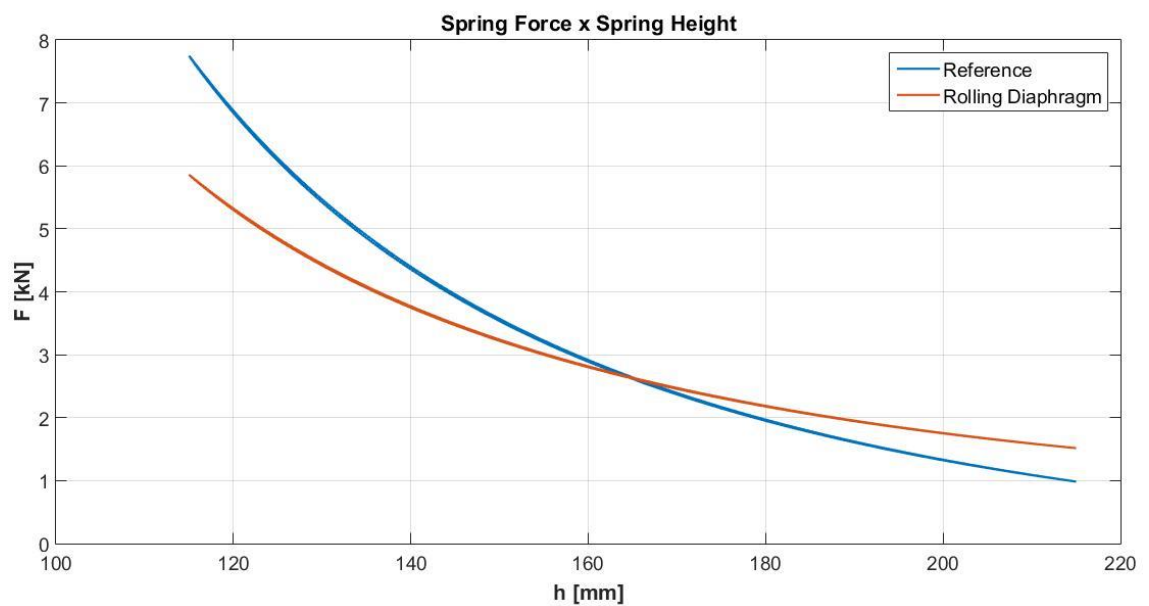


Figure 53 - Spring Force x Spring Height for a rolling diaphragm spring

The results show that for a rolling diaphragm spring with the same volume and same area of the reference double bellows spring, the stiffness is lower as well as the generated force. Although the rolling sleeve provides a lower force, as it does not change its effective area during deformation, it means that the spring occupies a smaller space what is desirable for small car suspension proposes.

4.4 Hysteresis

A noticeable effect that occurs by using the valve system is the hysteresis. It can be noticed when the valve is opened, and we can assume that this effect is due to the airflow though the valve during the compression and extension of the spring. To demonstrate this effect, we can compare the previous results of the spring force, stiffness and pressure behaviour, which were obtained with the closed valve, with a 1mm and 2mm opened valve simulation. The next figures show this comparison results.

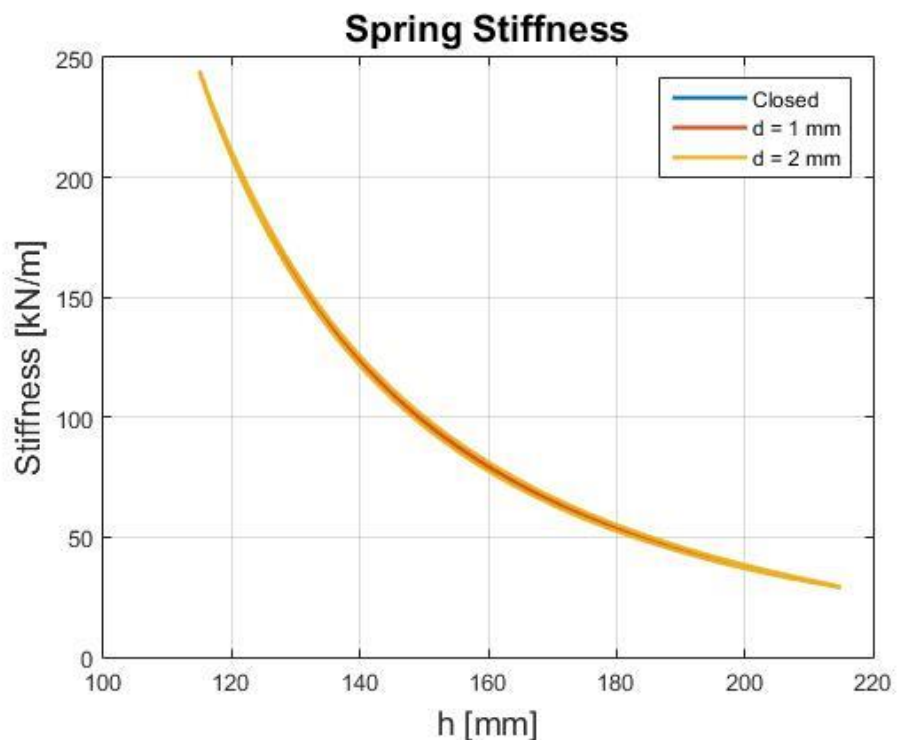


Figure 54 - Hysteresis effect: stiffness

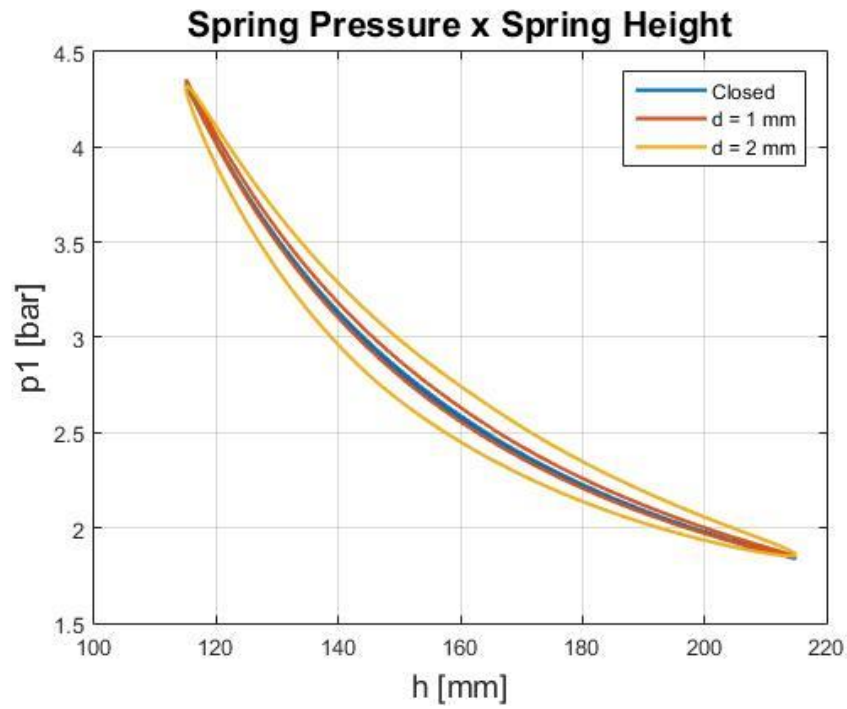


Figure 55 - Hysteresis effect: spring pressure

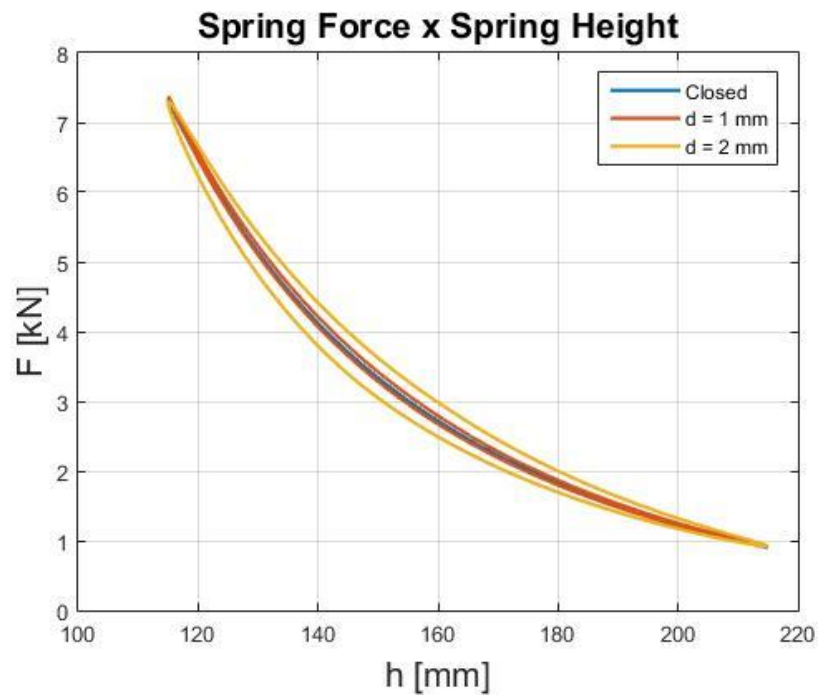


Figure 56 - Hysteresis effect: spring force

By comparing the results between the closed valve and the opened ones we realize that the hysteresis effect increases due to the valve opening. The spring stiffness present a slightly change so we can assign the force hysteresis due especially

to the hysteresis of the pressure behaviour. Thus, by using the auxiliary reservoir the hysteresis effect is something to take into account and must be mitigated.

4.5 Air tank analysis

In this section, the results of the simulations with the air tank are discussed. By using the models shown by Figure 33 and by Figure 34 we could calculate the time delay needed to fulfil the air spring so it could provide the required force.

First, only a study of the air spring being filled was done, so it was used a simpler model without a compressor. Thus, to compare the impact of the air tank pressure in the time needed to fill the air spring, two tank types were chosen, one with 13.79 Bar and the other with 10.34 Bar, both with a volume of 1.89 L. The result is shown by Figure 57.

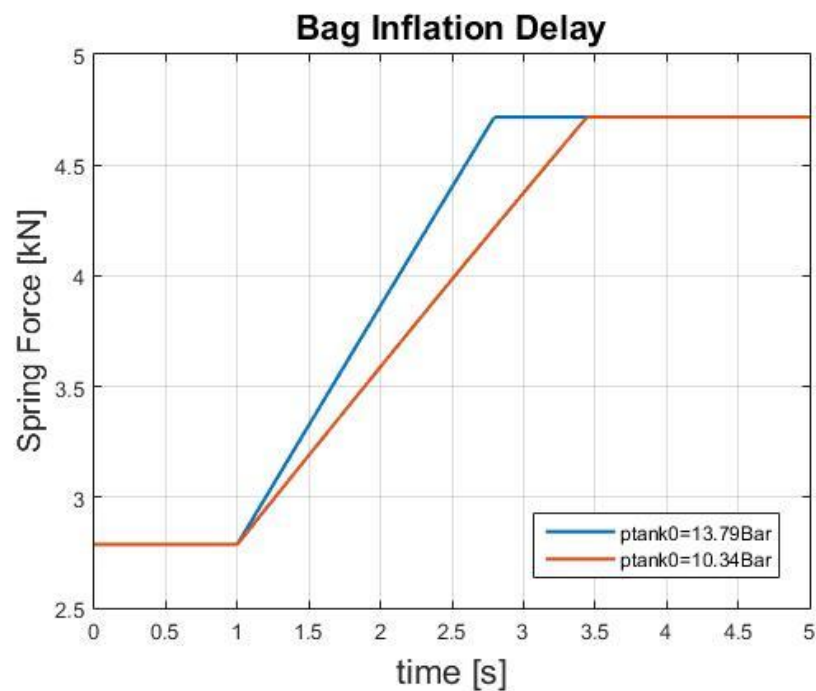


Figure 57 - Air spring inflation delay

The graph shows that for a higher pressure tank the time needed to fulfil the air spring decreases, what is expected since the airflow rate is given by the difference of pressure between the air spring and the air tank as evidenced by equation [35].

In order to expand this analysis for other types of tanks, some tank data was chosen from the market. The models were chosen so the tanks could fit in a city car, and the new results are given by Figure 58.

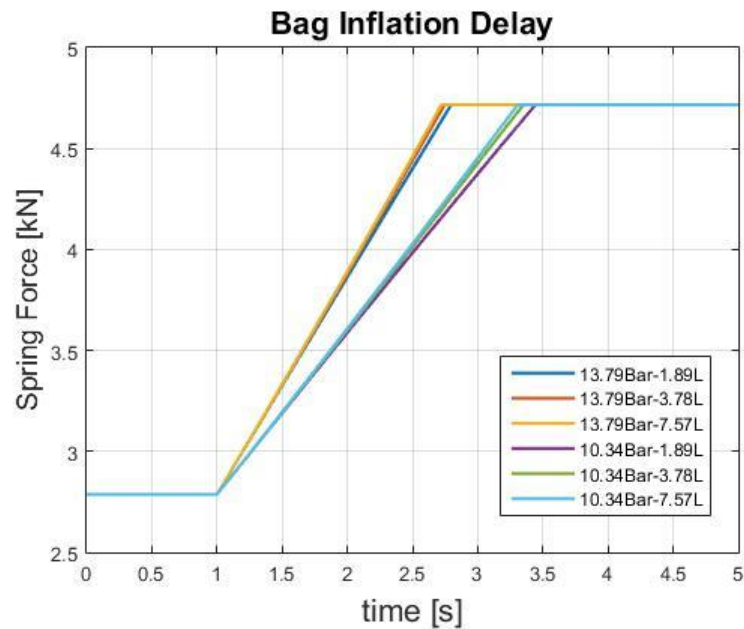


Figure 58 - Air spring inflation delay for different air tank types

According to the previous graph, one can see that what makes a considerable impact on time delay is the tank pressure. Table 4 highlight this time delay.

Table 4 - Air tank data with time delay

Tank	Pressure (Bar)	Volume (L)	Time Delay (s)
1	13.79	1.89	1.8
2		3.78	1.75
3		7.57	1.72
4	10.34	1.89	2.4
5		3.78	2.35
6		7.57	2.3

Thus, by analysing Figure 58 and Table 4 we can consider that the tank volume has a negligible impact on the time needed to fulfil the air spring. However, the air tank volume is important in terms of tank pressure loss as shown by Figure 59.

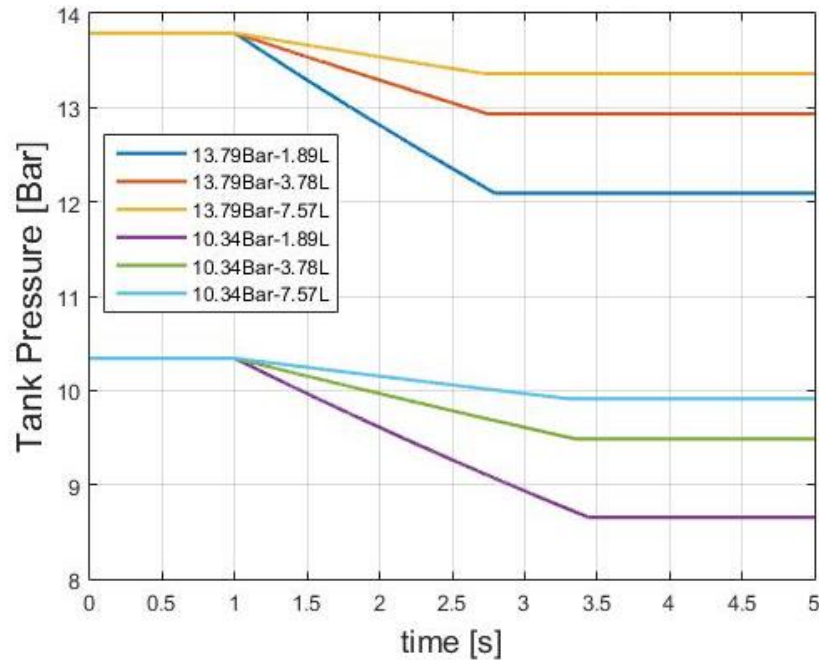


Figure 59 - Air tank pressure loss

One can realize that for smaller tank volumes the pressure loss is higher, what is an issue in cases of consecutive required forces. In these cases, for a second force input, the new initial tank pressure will be smaller, and for smaller tanks it will be much smaller, what increases the inflation delay considerably.

Considering that for a small city car, that is the focus of this project, a smaller tank is desirable, the recommended pressure would be the one of 13.79 Bar which guarantees the minimum inflation delay and the volume could be of 3.78 L, since the one of 1.89 L could be an issue in the case of consecutive forces and the one of 7.57 L presents dimensions issues for a small city car.

In the real project, the air system includes the air compressor which will fulfil the air tank, thus the effect of the compressor in relation to inflation delay was also studied. Figure 60 shows the pressure behaviour when using a compressor during the process of fulfilling the air spring.

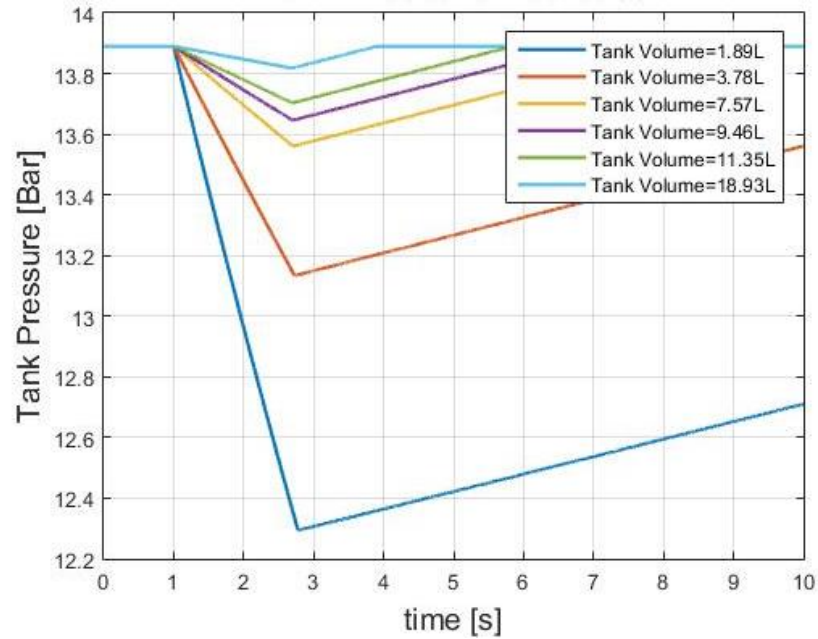


Figure 60 - Tank fulfil delay

As told before, for smaller tanks, the pressure loss is higher, so the time to fulfil the tank would be higher. Considering that for the Tank 2, which was chosen before, the pressure loss has a small impact for the system behaviour, there is no need to choose a higher volume tank just because of the smaller fulfilling time.

Table 5 - Air tank with compressor

Tank	Pressure (Bar)	Volume (L)	Time Delay (s)
7	13.79	1.89	1.78
8		3.78	1.73
9		7.57	1.7
10		9.46	1.7
11		11.35	1.7
12		18.93	1.69

Comparing Table 4 and Table 5, one can see that the time delay difference is quite negligible, thus we can assume that the compressor size and power has impact only on the fulfilling time of the air tank. Again, the dimensions of the compressor must be chosen according to a small city car dimensions limit.

It is important to highlight that this time delay calculated is considered very high for an active system, however, this depends especially on the airflow rate. Since the goal of this analysis is not to find the best valve or best airline that provides the best airflow, the results are evaluated just for comparative purposes.

4.6 Control Strategy: First approach

In this section it will be discussed the results of the proportional valve and the active configuration under a step input. First, to demonstrate the working principle of the valve, Figure 61 shows the relation between the spool displacement and the valve effective area.

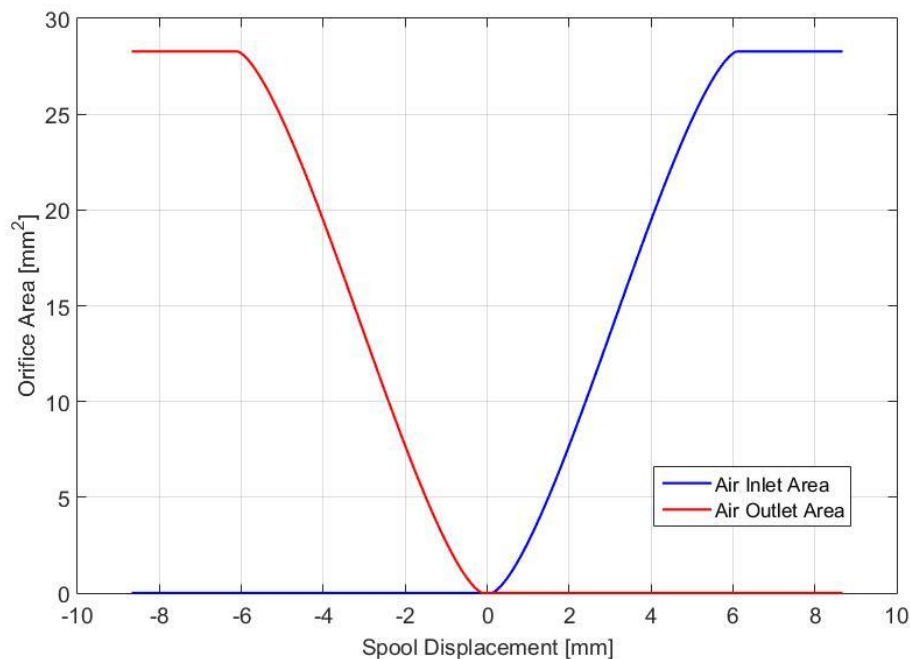


Figure 61 - Proportional valve working principle

The simulation above was done for a sinusoidal current input with 0.5 A of amplitude. As expected, when the inlet area is opened the outlet area is closed, and vice versa. With this result, the valve model could be implemented in the quarter car active model to analyse the effects of the proportional valve on the system and to see the availability of this control strategy.

As explained in section 3.6, there were two models simulated: one without the control valve and another with it. First, we will analyse the model without the valve and its results under a step input simulation of 50 mm are presented by Figure 62.

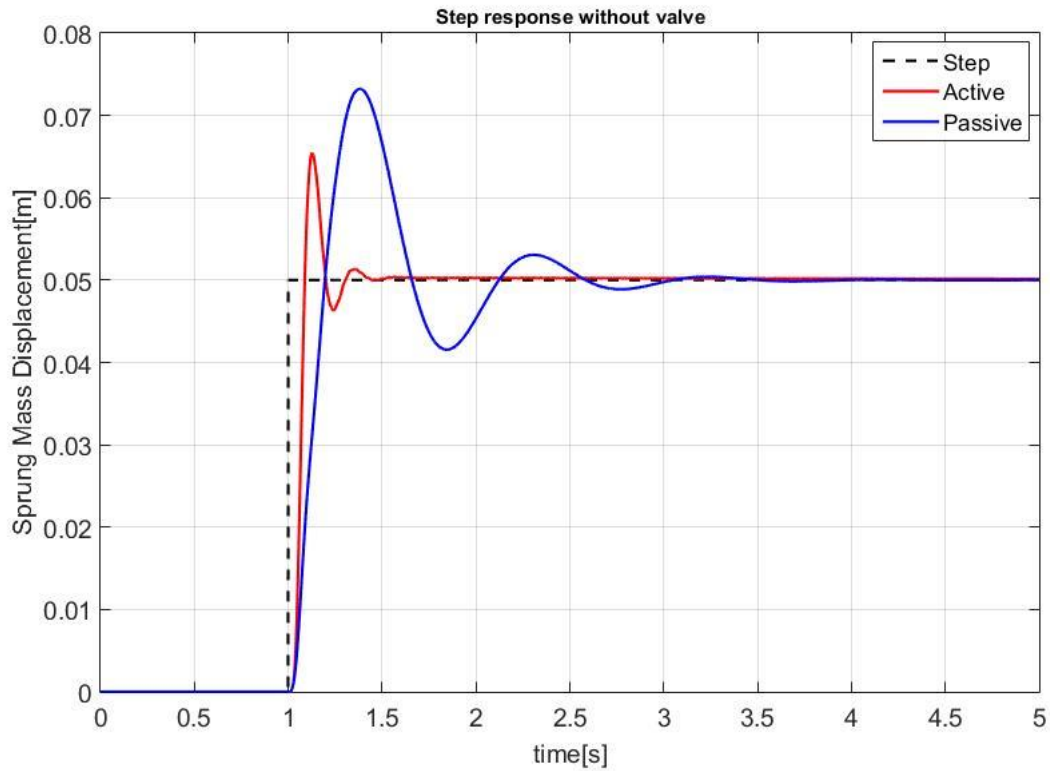


Figure 62 - Active system step response without control valve

One can see that the peak was decreased from approximately 0.074 m to 0.065 m and the settling time was much smaller, approximately 1.6 s. This kind of result can show that the system is working correctly, so the air spring can be used as an actuator when connected to a power source. Now, the active configuration is ready to the valve implementation, thus, by including the valve in the system, the new result for the same step input is given by Figure 63.

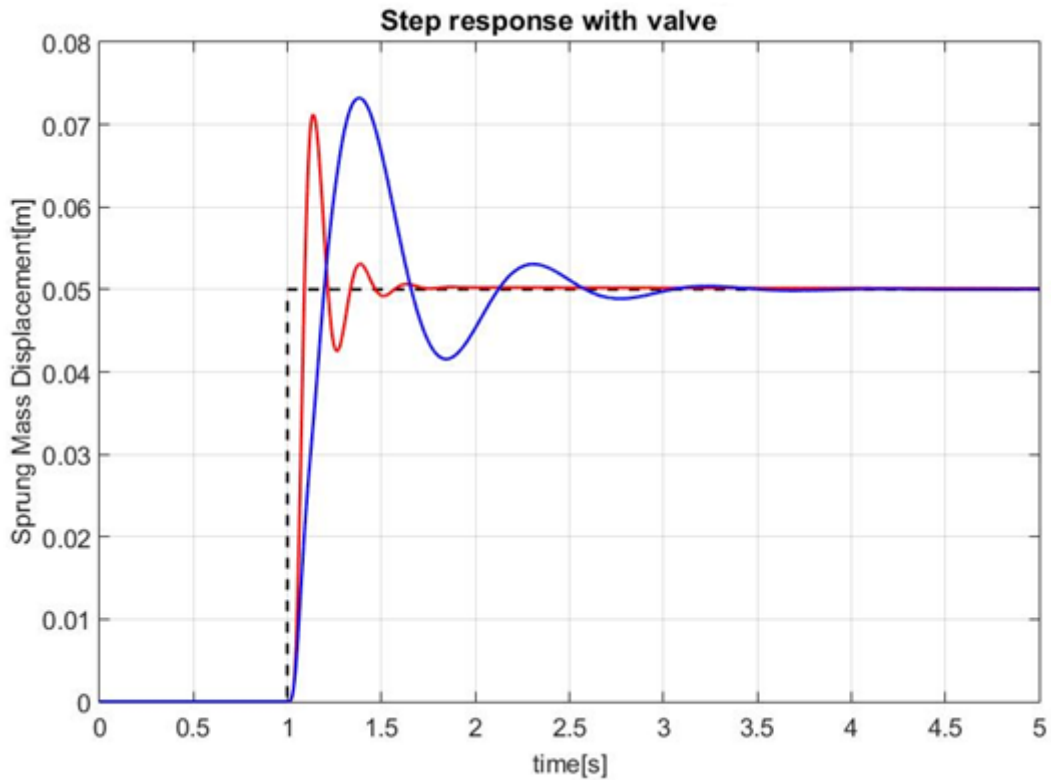


Figure 63 - Active configuration step response with valve

In this case, the peak is slightly higher (higher than 0.07 m) which is undesirable, and the system presents more oscillations with a slightly higher settling time.

The active configuration results show that the valve was successfully modelled and that the air spring can be used as an actuator and it improves the step response of the vehicle. Besides lowering the settling time, it also lowers the amplitude peak, however there are other control strategies to be verified that can bring different results for this type of solution and they were not explored on this project.

Finally, just for a matter of clarification, Figure 64 shows the pneumatic strut used on the simulations:

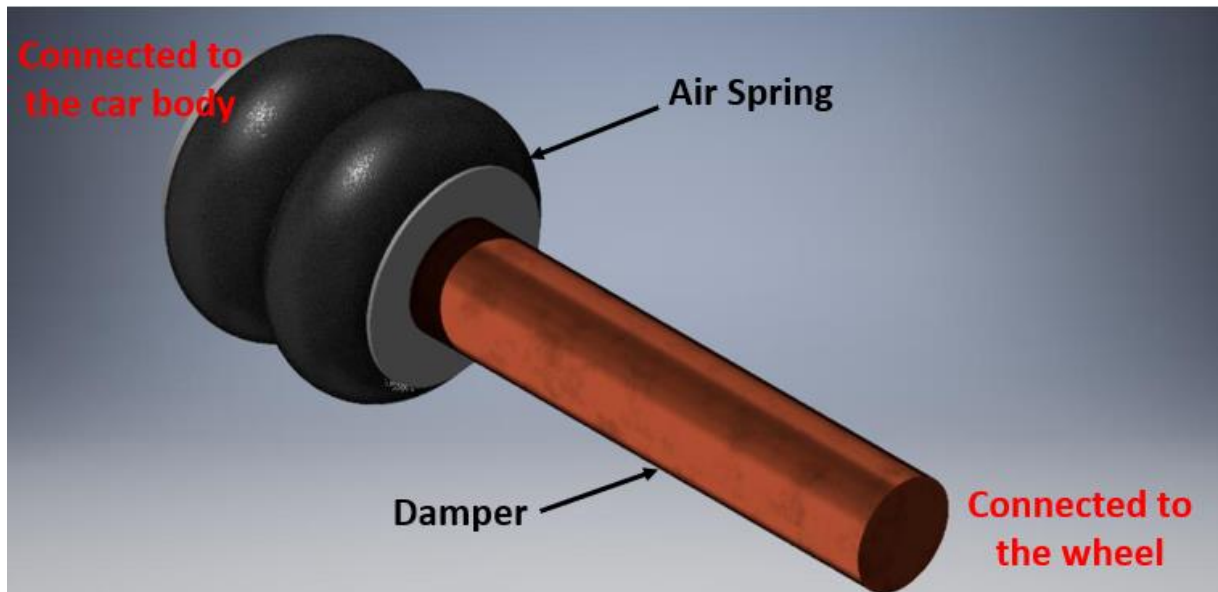


Figure 64 - Air suspension strut

Figure 64 presents the solution used, an air spring instead a mechanical spring, assembled with a damper.

5 Conclusion

After studying a large amount of literature in the pneumatic suspension field, the dynamic equations were developed, and the models was implemented on MATLAB-Simulink. The air spring alone was simulated and validated based on the literature, after that it was implemented on the air tank model and the active model.

With the validated model it was possible to determine the behavior of the air spring characteristics as stiffness, force and pressure. The calculated force is in line with the small city car required force as the maximum obtained with the simulated air spring was higher than the force value for a car under an acceleration of 2.5g. If the value for this kind of spring is not enough the effective area or the volume of the spring could be changed so the requirements are fulfilled. It was demonstrated the effects of changing the design parameters: the air spring volume and the air spring effective area. Increasing both parameters will increase the spring force, however the spring must obey the small city car constraints, so there is a limit. For the effective area, it was shown that a special type of air spring, called rolling diaphragm spring, does not present change of this parameter during compression and extension what can be considered an advantage since it simplifies the calculations.

In the section 4.4 it was presented the effect of the hysteresis that must be considered in the real project. It happens when the valve orifice reduces, increasing the air resistance as well as the hysteresis effect. It can be an issue to the control system of the vehicle since the values of measured and calculated forces can be different from expected, and this could forfeit the system performance. The hysteresis can be mitigated by using equipment with low friction.

After analyzing the spring alone, the model with an air tank was introduced. The results showed the time delay to inflate the bag under a specified external force and after that introduced a compressor to demonstrate its effects on the system. The objective was just to analyze the air tanks and how their parameters could impact on the time delay. It was concluded that the spring inflates faster when connected to bigger tanks or when connected to tanks with high pressures. Since the dimension limits must be respected the Tank 2 was selected as a valid option for a small city car

since it presents lower inflation time due to its high pressure and it presents a suitable volume. The addition of the compressor to the system is quite negligible to the calculations since it slightly impacts on the inflation time. However, it was demonstrated that for bigger tanks, the time to refill the tank can be an issue in cases of consecutive external forces actuating on the suspension.

Finally, the model of proportional valve was implemented and validated based on the literature and it was used for an active configuration of a quarter car model. For this active system, a model without the valve was done with a PID controller actuating on the airflow rate, what was used to confirm the reliability of the air spring as an actuator. After that, the proportional valve was implemented and the PID controller started actuating on the coil current that controls the valve spool. The model showed similar results to the previous one. It is important to highlight that this was a first approach of one type of control strategy and that there are more to be explored to find an optimum one. As the focus of this project is just to do a general analysis of the air spring, the PID control strategy was applied just to show the availability of this solution.

Therefore, according to the results the air spring can be used to replace the mechanical spring, since it provides the required force for a small city car, its dimensions respect the project constraints and it improves the step response as an active system.

For future projects it is suggested to focus on other types of control strategies and, by using this model, to explore an optimum shape for a small city car.

6 Bibliography

- Air Lift Company*. (n.d.). Retrieved from <http://www.airliftcompany.com>
- Bachrach, B. I., & Rivin, E. (1983, August 24). Analysis of a Damped Pneumatic Spring. *Journal of Sound and Vibration* , pp. 191 - 197.
- Barata, J. (2016, February 10). *Flatout*. Retrieved from <https://www.flatout.com.br/o-que-era-e-que-fim-levou-a-misteriosa-suspensao-ativa-da-bose/>
- Beater, P. (2007). Pneumatic Drives. *System Design, Modeling, and Control*.
- Ben-Dov, D., & Salculean, S. E. (1995). A Force-Controlled Pneumatic Actuator. *IEEE Trans. Rob. Autom.*, 906–911.
- Cavanaugh, R. D. (1961). Air Suspension and Servo-Controlled Pneumatic Isolation Systems. In *Shock and Vibration Handbook*. McGraw - Hill B. C.
- Chang, F., & Lu, Z.-H. (2008). Dynamic model of an air spring and integration into a vehicle dynamics model. *Proceedings of the Institution of Mechanical Engineers*, pp. 1813-1825.
- Dunlop*. (n.d.). Retrieved from <https://www.dunlopsystems.com/product-range>
- Ebrahimi, B. (2009). Development of Hybrid Electromagnetic Dampers for Vehicle Suspension Systems. *PhD Theses*. Waterloo, Ontario.
- Elbeheiry, E. M., Karnopp, D. C., Elaraby, M. E., & Abdelraaouf, A. M. (1995). Advanced Ground Vehicle Suspension Systems - A Classified Bibliography. *Vehicle System Dynamics: International Journal of Vehicle Mechanics and Mobility*, pp. 231 - 258.
- Esmailzadeh, E. (1978, July). Optimization of Pneumatic Vibration Isolation System for Vehicle Suspension. *ASME*, pp. 500 - 506.
- F1 Dictionary*. (n.d.). Retrieved from http://www.formula1-dictionary.net/damper_magnetorheological.html

- Firestone. (n.d.). *Airide Design Guide - Suspension Applications*. Firestone industrial Products Company.
- Genta, G., & Morello, L. (2009). *The Automotive Chassis - Volume 1: Components Design*. Torino: Springer.
- Gysen, B. L., Paulides, J. J., Janssen, J. L., & Lomonova, E. (2010, January 01). Active Electromagnetic Suspension System for Improved Vehicle Dynamics. *IEEE Transactions on Vehicular Technology*.
- Kornhauser, A. A., & Smith, J. L. (1993). The effects of Heat Transfer on Gas Spring. *Journal of Energy Resource Technology*, 70-75.
- Lallo, M. D. (2016, July 28). *Auto Supermarket*. Retrieved from <http://www.autosupermarket.it/magazine/le-sospensioni-attive-e-adattive-di-mercedes/>
- Lee, S. J. (2010). Development and Analysis of an Air Spring Model. *International Journal of Automotive Technology*, 471-479.
- Li, H., Guo, K., Chen, S., WeiWang, & Cong, F. (2013). *Design of Stiffness for Air Spring Based on ABAQUS*. Hindawi Publishing Corporation.
- M3 Post. (n.d.). Retrieved from <https://www.m3post.com/forums/showthread.php?t=1345149>
- Milliken, W. F., & Milliken, D. L. (1995). *Race Car Vehicle Dynamics*. Warrendale : SAE International .
- Moran, M. J., & Shapiro, H. N. (2006). *Fundamentals of Engineering Thermodynamics*. The Atrium, Southern Gate, Chichester West Sussex PO19 8SQ, England: John Wiley & Sons Ltd.
- Ogata, K. (2002). *Modern Control Engineering*. Upper Saddle River, New Jersey: Prentice-Hall, Inc.

- Process & Pneumatics*. (n.d.). Retrieved from <http://www.processpneumatics.com/applications/air-ride-suspension-systems/>
- Quaglia, G., & Sorli, M. (2000, August). Experimental And Theoretical Analysis Of An Air Spring With Auxiliary Reservoir. *Proc. of the 6th Internationales Symposium on Fluid Control*.
- Quaglia, G., & Sorli, M. (2001). Air Suspension Dimensionless Analysis and Design Procedure. *Vehicle System Dynamics*, 443 - 475.
- Richer, E., & Hurmuzlu, Y. (2000). A High Performance Pneumatic Force Actuator System: Part I - Nonlinear Mathematical Model. *JOURNAL OF DYNAMIC SYSTEMS, MEASUREMENT, AND CONTROL*, 416-425.
- Robinson, W. D. (2012). A pneumatic semi-active control methodology for vibration control of air spring based suspension systems. *PhD Theses*. Ames, Iowa.
- Sanville, F. E. (1971). A New Method of Specifying the Flow Capacity of Pneumatic Fluid Power Valves. *Second International Fluid Power Symposium*, 37-47.
- Sharp, R. S., & Hassan, J. H. (1988). Performance Predictions for a Pneumatic Active Car Suspension System. *Proceedings of the Institution of Mechanical Engineers*, 202, pp. 243 - 250.
- SpeedWay Motors*. (n.d.). Retrieved from <https://www.speedwaymotors.com/Tru-Coil-Street-Stock-Racing-Coil-Springs-Front-5-1-2-x-12-Inch,166.html>
- Toyofuku, K., Yamada, C., Kagawa, T., & Fujita, T. (1999). Study on Dynamic Characteristic Analysis of Air Spring with Auxiliary Chamber. *JSAE*, pp. 349-355.
- W220 - Airmatic*. (n.d.). Retrieved from <https://w220.ee/Airmatic>
- Winnen, A. (2005). *Aufbau eines Luftfedermodells dūr die simulationsprogramme MATLAB/Simulink und ADAMS/CAR*. Aachen, Germany: Faculty of Mechanical Engineering, Aachen University of Technology.